Naval Research Laboratory

Washington, DC 20375-5320

NRL/MR/6300--12-9414

Extraction of Carbon Dioxide and Hydrogen from Seawater by an Electrochemical Acidification Cell Part III: Scaled-up Mobile Unit Studies (Calendar Year 2011)

HEATHER D. WILLAUER

Materials Science and Technology Division

DENNIS R. HARDY

Nova Research Inc.
Alexandria, Virginia

FREDERICK W. WILLIAMS

Navy Technology Center for Safety and Survivability
Chemistry Division

FELICE DIMASCIO

Office of Naval Research
Arlington, Virginia

May 30, 2012

REPORT DOCUMENTATION PAGE

Form Approved
OMB No. 0704-0188

1. REPORT DATE *(DD-MM-YYYY)*	2. REPORT TYPE	3. DATES COVERED *(From - To)*
30-05-2012	Memorandum Report	

4. TITLE AND SUBTITLE

Extraction of Carbon Dioxide and Hydrogen from Seawater by an Electrochemical Acidification Cell Part III: Scaled-up Mobile Unit Studies (Calendar Year 2011)

5a. CONTRACT NUMBER

5b. GRANT NUMBER

5c. PROGRAM ELEMENT NUMBER

6. AUTHOR(S)

Heather D. Willauer, Dennis R. Hardy,* Frederick W. Williams, and Felice DiMascio†

5d. PROJECT NUMBER

5e. TASK NUMBER

5f. WORK UNIT NUMBER
63-9189-0-1-5

7. PERFORMING ORGANIZATION NAME(S) AND ADDRESS(ES)

Naval Research Laboratory, Code 6300
4555 Overlook Avenue, SW
Washington, DC 20375-5320

8. PERFORMING ORGANIZATION REPORT NUMBER

NRL/MR/6300--12-9414

9. SPONSORING / MONITORING AGENCY NAME(S) AND ADDRESS(ES)

Office of Naval Research
One Liberty Center
875 North Randolph Street, Suite 1425
Arlington, VA 22203

10. SPONSOR / MONITOR'S ACRONYM(S)

ONR

11. SPONSOR / MONITOR'S REPORT NUMBER(S)

12. DISTRIBUTION / AVAILABILITY STATEMENT

Approved for public release; distribution is unlimited.

13. SUPPLEMENTARY NOTES

*Nova Research Inc., Alexandria, VA
†Naval Reserve Officer, Program 38, Office of Naval Research, Arlington, VA

14. ABSTRACT

An electrochemical acidification cell was developed and tested as a method for extracting large quantities of CO_2 from seawater for use as a feedstock for jet-fuel synthesis at sea. After the technology was successfully demonstrated in the laboratory, it was scaled-up and integrated into a mobile skid design. This report details the results of four separate evaluations (January 22–27, April 25–29, July 11–15, August 28–September 1) of the electrochemical acidification cell performance as a function of pH, current, time, polarity reversal, and CO_2 and H_2 recovery.

15. SUBJECT TERMS

Electrochemical acidification cell
Carbon dioxide
Hydrogen
Polarity reversal

16. SECURITY CLASSIFICATION OF:			17. LIMITATION OF ABSTRACT	18. NUMBER OF PAGES	19a. NAME OF RESPONSIBLE PERSON
a. REPORT	b. ABSTRACT	c. THIS PAGE			Heather D. Willauer
Unclassified Unlimited	Unclassified Unlimited	Unclassified Unlimited	Unclassified Unlimited	41	19b. TELEPHONE NUMBER *(include area code)* (202) 767-2673

Standard Form 298 (Rev. 8-98)
Prescribed by ANSI Std. Z39.18

CONTENTS

EXECUTIVE SUMMARY

A sea-based synthetic fuel process that combines carbon dioxide (CO_2) and hydrogen (H_2) to make jet fuel at sea is envisioned. However before such a process can become feasible, methods must be developed to extract large quantities of CO_2 and H_2 from seawater fast and efficiently. To this end, commercially available electrodeionization cells have been modified by NRL to function as electrochemical acidification cells. After the technology was successfully demonstrated in the laboratory, it was scaled-up and integrated into a mobile skid design. The skid was constructed and pre-tested at Havlovick Engineering Services in Idaho Falls, Idaho before it was sent to NRL Key West on January 21, 2011 to be evaluated in a marine environment. This report details the results of four separate evaluations (January 22th – 27th, April 25th – 29th, July 11th – 15th, August 28th – Sept 1st) of the electrochemical acidification cell performance as a function of pH, current, time, polarity reversal, and CO_2 and H_2 recovery. The results show that the cell was successfully scaled-up, incorporated into a mobile platform, and operated efficiently during four separate evaluations. The electrical resistance profiles show that cyclically reversing the polarity of the cell's electrodes minimizes the effects of mineral and organic deposits on the electrode surface. The pH profiles illustrate that the acidification cell reproducibly reduces seawater pH below 6.0. From these data, a set of times were determined to provide operational parameters for the cell. Quantitative measurements by coulometry confirmed CO_2 extraction from the cell at 92% using hollow fiber membrane technology. H_2 production from the cathode was qualitatively confirmed at different applied cell currents by a gas analyzer.

EXTRACTION OF CARBON DIOXIDE AND HYDROGEN FROM SEAWATER BY AN ELECTROCHEMICAL ACIDIFICATION CELL
PART III: SCALED-UP MOBILE UNIT STUDIES (CALENDAR YEAR- 2011)

1.0 BACKGROUND

The feasibility of producing jet fuel at sea from environmental CO_2 and H_2 to support carrier flight operations is of interest. In-theater, synthetic fuel production is a "game changing" proposition that could offer the Navy significant logistical and operational advantages by reducing dependence on increasingly expensive fossil fuels and by reducing fuel logistic tails and their vulnerabilities resulting from fuel delivery at sea. The Navy has proposed moving to a common fuel JP5, throughout its operations [1]. Petroleum derived fuel cost and availability issues have prevented this transition so far. If the Navy does move to a single fuel this proposed process would simplify any future shipboard production of fuel. In addition, a ship's ability to produce any significant fraction of the battle group's fuel for operations would increase the Navy's operational flexibility and time on station by reducing the mean time between refueling.

Technologies currently exist to synthesize hydrocarbon fuel on land, given sufficient primary energy resources such as coal [2]. However, these technologies are not CO_2 neutral, and they are not practical for a sea-based operation. Extracting CO_2 from seawater is part of a larger project to create liquid hydrocarbon fuel at sea [3-10].

One part of the overall program by NRL (Naval Research Laboratory) was a series of tests in the laboratory to recover CO_2 and H_2 from seawater using an electrochemical acidification cell [11]. The objective of those studies was to determine the effects of acidification cell configuration, seawater composition, flow rate, and current on seawater pH.

Exploiting seawater's pH is an indirect approach to recovery of CO_2 in the form of bicarbonate from the equilibrium conditions of CO_2 in seawater as shown in equations 1 and 2 [12]. The protons generated in the process acidify the seawater from pH 7.8 to pH 6.0. Johnson, et al demonstrated that when the pH of seawater is decreased to 6 or less, carbonate and bicarbonate are re-equilibrated to CO_2 gas as shown in equation 3. This method has been the basis for standard quantitative ocean $[CO_2]_T$ measurements for over 25 years [12].

$$[CO_2(g)]_{air} \overset{H_2O}{\rightleftarrows} [CO_2(aq)] \overset{H_2O}{\rightleftarrows} [H_2CO_3(aq)] \quad (1)$$

$$CO_2(g) \overset{H_2O}{\rightleftarrows} CO_2(aq) \overset{H_2O}{\rightleftarrows} H_2CO_3(aq) \rightleftarrows 2HCO_3^-(aq) \rightleftarrows CO_3^{2-}(aq) + H_2O(l) + CO_2(g)\uparrow \quad (2)$$

$$HCO_3^- + H^+ \rightleftarrows H_2CO_3 \rightleftarrows H_2O + CO_2(g)\uparrow \quad (3)$$

Manuscript approved March 9, 2012.

NRL laboratory studies have shown that the acidification cell was able to decompose freshwater in the electrode compartments into hydrogen ions (H^+), hydroxyl ions (OH^-), H_2 gas, and oxygen gas (O_2) by means of electrical energy. Simultaneous and continuous ion exchange and regeneration occurred within the cell eliminating the need for regeneration by caustic chemicals. The degree of ion exchange and regeneration within the cell was controlled by the applied current. Lowering the pH of seawater by the acidification cell was found to be an electrically driven process, where seawater pH is proportional to applied current. In addition to CO_2, the cell produced a portion of the H_2 needed for a hydrocarbon synthesis process with no additional energy penalty. The acidification cell operated in the laboratory at a seawater flow rate of 140 mL/min and both electrode compartments at a deionized water flow rate of 10 mL/min [11].

2.0 OBJECTIVE

The objective of this phase of the overall project has been to transition the technology from the laboratory to a marine environment for the purpose of scaling-up and integrating the processes. In this environment, CO_2 and H_2 can be produced in quantities far above those achieved at the laboratory scale. The electrochemical acidification cell for these test series has been scaled-up to operate at a minimum seawater flow rate of 0.5 gal/min (1,900 mL/min) and a minimum electrode compartment flow rate of 0.06 gal/min (230 mL/min), and the cell has been designed as an integral part of a mobile platform unit. The following key technological challenges associated with scaling-up were addressed:

- System component sustainability
- Heat generation in the acidification cell
- Ion exchange and system regeneration
- Process efficiencies
- Membrane fouling
- Mineral deposition on the electrodes
- Power requirements
- Hydrogen production
- CO_2 recovery

3.0 APPROACH

In these test series an electrochemical acidification carbon capture skid was operated at NRL's Marine Corrosion Facility in Key West, Florida on four separate occasions (January 22th – 27th, April 25th – 29th, July 11th – 15th, August 28th – Sept 1st) to evaluate and optimize key technological parameters associated with recovering CO_2 and H_2 fast and efficiently from seawater.

4.0 TEST DESCRIPTION

4.1 Electrochemical Acidification Cell

A standard commercially available electrodeionization cell (Ionpure LX-X Module) was modified to function as an electrochemical acidification cell for this evaluation. Although its design is not optimized for use as an acidification cell, it has more than served the purpose in this

study. A custom design will be required to optimize the existing cell's performance. In addition a custom design will be needed for any future larger scale-up studies that will involve seawater flow rates greater than 5,700 mL/min.

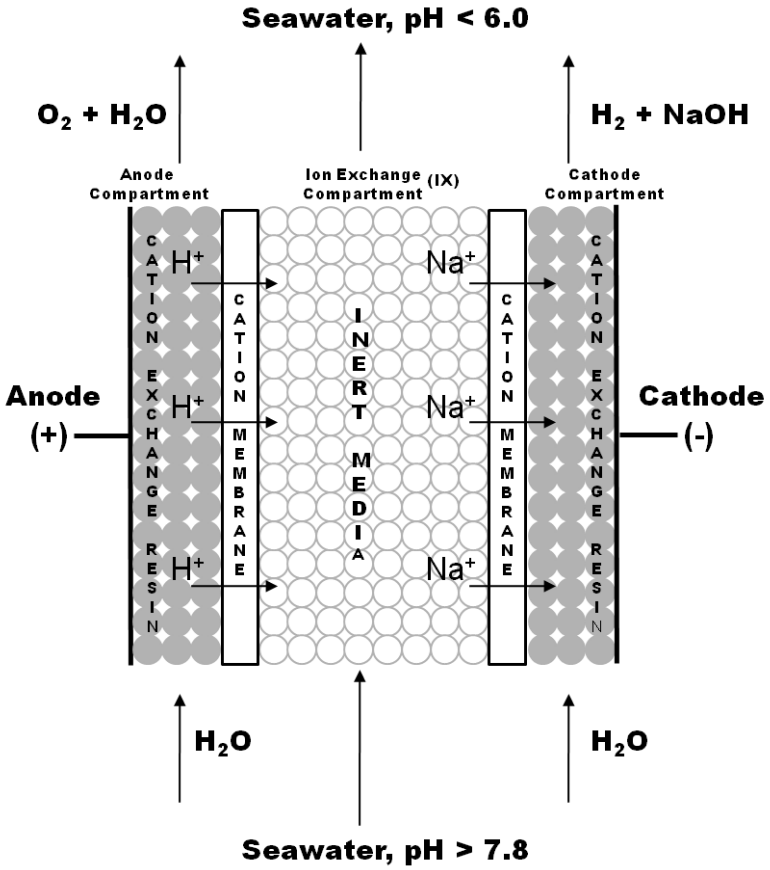

← Electrons travel from cathode to anode in external circuit
Positive ions travel through solution from anode to cathode→

Figure 1. Schematic of Electrochemical Acidification Cell

The major components of an acidification cell include a central ion exchange (IX) compartment, electrode compartments (cathode and anode) and cation-permeable membranes which separate the three compartments. A cation-permeable membrane is a cross-linked polymer backbone with sulfonic acid groups attached. The acid functionality provided discrete channels for cations to migrate through the polymer matrix while blocking the passage of anions. Figure 1 shows a typical three compartment cell configuration.

Inert ceramic particles are used in the IX compartment to serve as a support structure for the membranes. In this compartment, the ions exchange in the liquid phase. In addition Figure 1 shows that the electrode compartments contained strong cation exchange resin (Rohm & Haas IR-120).

The acidification cell in Figure 1 uses direct current (DC) to exchange sodium ions (Na^+) for H^+ ions in a central stream that is flowing adjacent to two cation exchange membranes. Seawater is passed through the center compartment of the three compartment cell. Na^+ ions are transferred through the membrane closest to the cathode and removed from the seawater by means of direct current (DC) voltage. These Na^+ ions are replaced by H^+ ions as the current drives the ions through the membrane closest to the anode to acidify the seawater.

Table 1. Cell Configured as an Electrochemical Acidification Cell

Dimensions	
Approximate Overall Cell Dimension	33 cm x 61 cm x 16 cm
IX Compartment Width	14 cm
IX Compartment Height	35.5 cm
IX Compartment Thickness	1.8 cm
IX Compartment Volume	895 cm^3
Membranes Active Area	497 cm^2 (each)
Each Electrode Compartment Volume	214 cm^3
Electrical Specification	
Electrode Active Area	497 cm^2 (each)
Max. Current Density	1,500 A m^{-2}
Flow Specification	
Max. Seawater Flow Rate	3900 mL/min
Operating Seawater Flow Rate	1900 mL/min
Max. RO Electrolyte Flow Rate	2100 mL/min
Operating RO Flow Rate	230 mL/min
Max. Operating Temperature	60 ^oC
Max. Operating Pressure	350 kPa
Materials	
Anode	Platinized Titanium
Cathode	Platinized Titanium
Membrane	Ionpure Cation-Permeable Membrane
Molded Frame and End Block	Polyethylene (PE)

In the cell, the anolyte is the water fed to the anode compartment. At the anode H^+ is generated and it must migrate from the surface of the anode, through the cation-permeable membrane, and into the IX compartment where it replaces Na^+. Therefore the anolyte was diluted such that H^+ ions are in excess and do not compete with any other cations. Water with a conductivity of less than 200 µS/cm, such as reverse osmosis (RO) permeate, is required.

The catholyte is the water fed to the cathode compartment and it must be free from hardness ions such as calcium (Ca^{+2}) and magnesium (Mg^{+2}). The pH in the cathode compartment is high enough to precipitate these hardness ions. Therefore, a total hardness concentration of less than 50 ppm, such as RO permeate, is required. As a part of these tests, the effects of RO permeate as the anolyte and catholyte were evaluated.

Table 1 provides a detailed description of the acidification cell's electrical and flow rate specifications along with the materials used in the cell configuration. The anode and cathode are platinum plated titanium electrodes. These tests determined the flow rate to current ratio required to lower seawater pH to the target level. This information determines electrode performance and operating life. The cell contained a polyethylene extruded cation permeable membrane. Membrane performance was evaluated during these tests, since its performance and operating life is based on current density and level of organic compounds contained in the seawater.

4.2 Electrochemical Acidification Cell Reactions

Figure 1 shows an acidification cell exchanging Na^+ for H^+ in a stream that is flowing adjacent to two cation-permeable membranes. Direct current (DC) facilitates this exchange. Depicting seawater by sodium chloride (NaCl) and acidified seawater by HCl, the reactions within the electrochemical acidification cell are as follows:

Anode: $2H_2O \rightarrow 4H^+ + O_2 + 4e^-$ (4)

IX: $4|NaCl|_{Seawater} + 4H^+ \rightarrow 4\,Na^+ + 4|HCl|_{Acidic\ Seawater}$ (5)

Cathode: $4H_2O + 4Na^+ + 4e^- \rightarrow 4NaOH + 2H_2$ (6)

Overall: $6H_2O + 4NaCl \rightarrow 4|HCl|_{IX} + 4|NaOH| + 2|H_2|_{Cathode} + |O_2|_{Anode}$ (7)

The amount of H^+ generated by the cathode is proportional to the applied electrical current, which follows Faraday's constant. Faraday's constant is defined as the amount of electricity associated with one mole of unit charge or electron, having the value 96,487 ampere-second/equivalent.

For the anode reaction, 96,487 A-sec will produce ¼ mole O_2 gas and 1 mole H^+ and for the cathode reaction, 96,487 A-sec will produce ½ mole H_2 gas and 1 mole OH^-. This allows the amount of H^+, OH^-, H_2, and O_2 produced per amp/second of current passed through the electrodes to be derived:

Anode Reaction

$$\left(\frac{1/4\ \text{mole}\ O_2}{96{,}487\ \text{A-sec}}\right)\left(\frac{60\ \text{sec}}{\text{min}}\right) = 0.000155\ \frac{\text{mole}\ O_2}{\text{A-min}} \quad (8)$$

$$\left(\frac{1\,\text{mole } H^+}{96{,}487\,\text{A-sec}}\right)\left(\frac{60\,\text{sec}}{\text{min}}\right) = 0.000622\,\frac{\text{mole } H^+}{\text{A-min}} \quad (9)$$

Cathode Reaction

$$\left(\frac{1/2\,\text{mole } H_2}{96{,}487\,\text{A-sec}}\right)\left(\frac{60\,\text{sec}}{\text{min}}\right) = 0.000311\,\frac{\text{mole } H_2}{\text{A-min}} \quad (10)$$

$$\left(\frac{1\,\text{mole } OH^-}{96{,}487\,\text{A-sec}}\right)\left(\frac{60\,\text{sec}}{\text{min}}\right) = 0.000622\,\frac{\text{mole } OH^-}{\text{A-min}} \quad (11)$$

Therefore, for seawater with a bicarbonate (HCO_3^-) ion concentration of 142 ppm (0.0023 M) at a planned operating flow rate of 0.5 gal/min (1900 mL/min), a theoretical applied current of 7.0 amps will be required to lower the pH to less than 6.0 and convert HCO_3^- to carbonic acid (H_2CO_3) (equation 12).

$$\frac{\left(\frac{0.0023\ \text{mole } HCO_3^-}{\text{Liter}}\right)\left(\frac{1.89\ \text{Liter}}{\text{min}}\right)}{\left(\frac{0.000622\,\text{mole } H^+}{\text{A-min}}\right)} = 7.0\,\text{A} \quad (12)$$

Removal efficiency can be defined as the ratio of the theoretical amount of CO_2 removed to the actual amount of CO_2 removed in the acidified seawater. The theoretical amount of CO_2 that can be removed from the acidified seawater is 0.0023 moles per liter. Removal efficiencies are never 100 % and can range from 50 to 95 % based on various unit operating requirements. The overall removal of CO_2 in these tests was measured to be approximately 92%.

The amount of H_2 gas generated at 7.0 A is

$$\left(\frac{1/2\,\text{mole } H_2}{96{,}487\,\text{A-sec}}\right)\left(\frac{60\,\text{sec}}{\text{min}}\right)(7.0\,\text{A}) = 0.0022\,\frac{\text{mole } H_2}{\text{min}} \quad (13)$$

Under these conditions, the molar ratio of H_2 to CO_2 is 0.73. Increasing the current increases the molar ratio of hydrogen to carbon dioxide with no effect on the operation of the acidification cell. H^+ generated will either exchange with Na^+ in the seawater to further lower its pH or migrate through the IX compartment and into the cathode compartment where it will combine with OH^- to form water.

4.3 Carbon Capture Skid

The acidification cell was mounted onto a portable skid along with an RO unit, power supply, pump, carbon dioxide recovery system, and hydrogen stripper to form a carbon capture system. Figures 2 and 3 are a composite schematic and picture of the system with dimensions of 63" x 36" x 60". Figure 4 provides a block diagram that describes how the system in Figure 2 operates. The system has evolved since its initial conception and installation at NRL Key West in January of 2011, to include different carbon recovery technology and more filtration media. Seawater is supplied to the skid by an in house 40 psi supply line. The water is filtered by two spin down filters in series (100 μm and 30 μm). After filtration a portion of the seawater is sent to an 11 gallon high density polyethylene container that functions as the seawater feed container. Before the seawater in the seawater feed tank is fed to the center compartment of the acidification cell at 0.5 gallon/minute, it is pumped through a 5 μm filter cartridge. The other portion of the seawater supply is fed to the RO system for processing. The RO system is an EPRO-1000SW from Crane Environmental, Inc. (Venice, FL) that is capable of producing 0.07 gallons per minute (1000 gallons per day) of permeate (potable water quality from seawater at a conductivity of approximately 200 μS/cm). This water is stored in an 11 gallon polyethylene container that is specified as the RO feed container (Figure 3). This water is the feed water to the electrode compartments of the acidification cell at a flow rate of 0.12 gallon/minute (460 ml/min). The flow is split as it enters the acidification cell resulting in electrode compartment flow rates of 0.06 gallon/minute (230 mL/min).

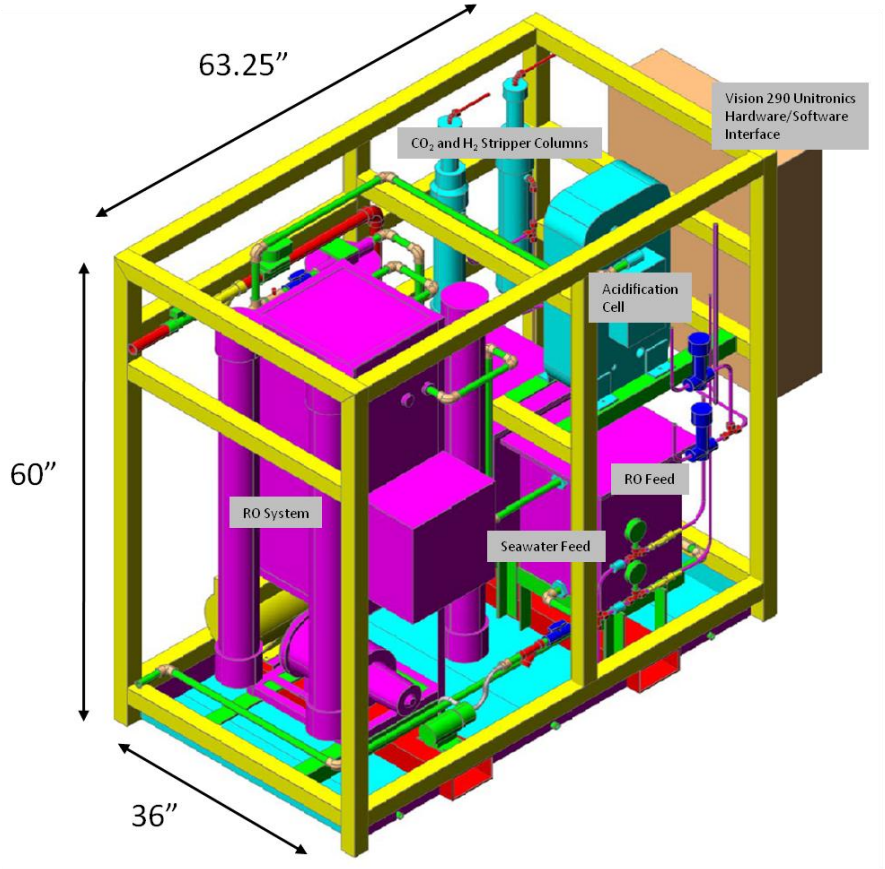

Figure 2. Composite Schematic of Carbon Capture Skid

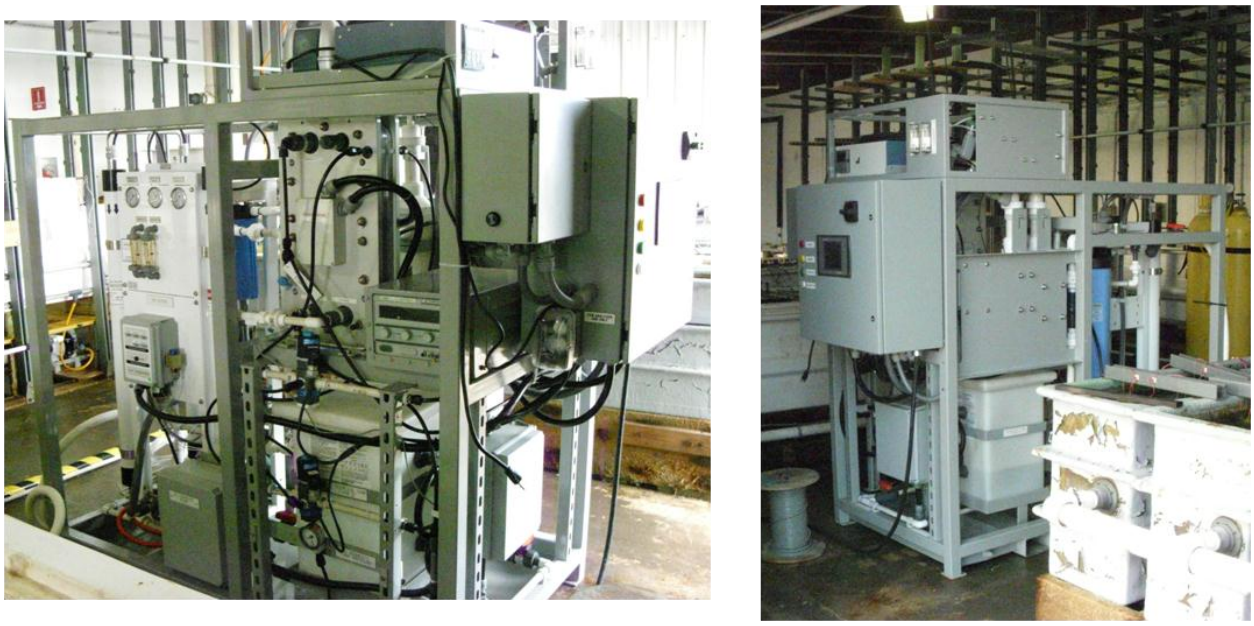

Figure 3a. Front and 3b. Back Pictures of Carbon Capture Skid at NRL Key West Facility

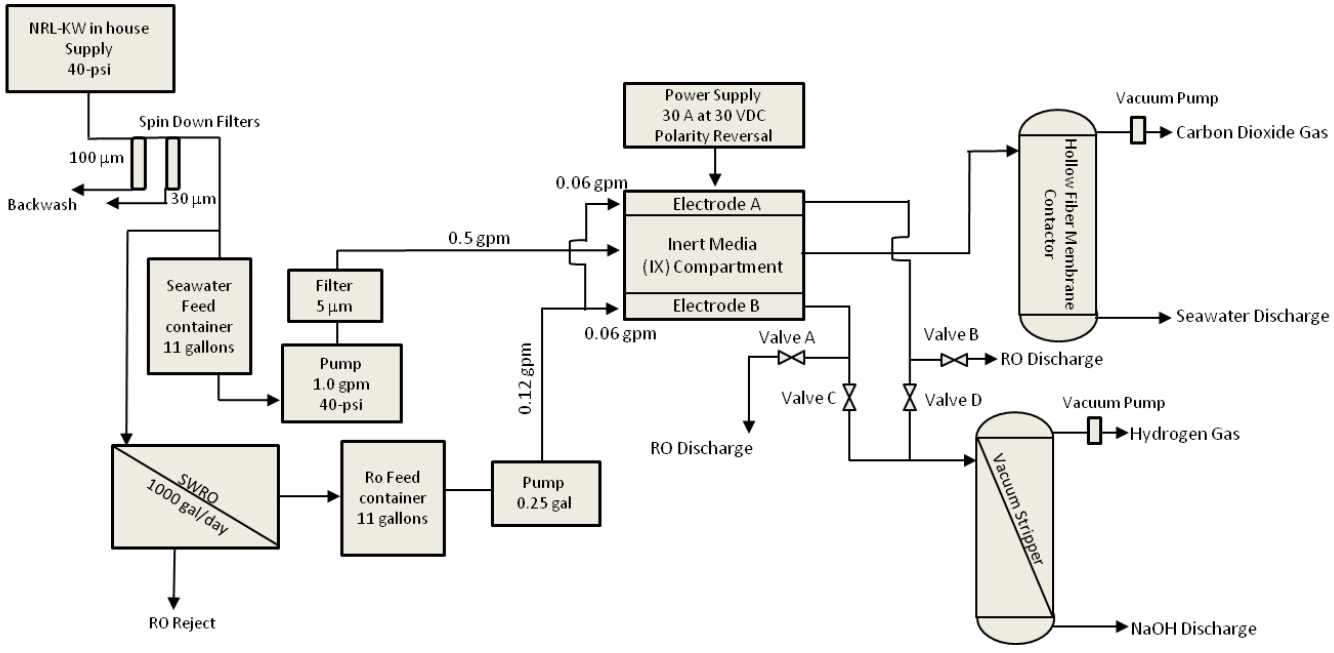

Figure 4. Block Diagram Carbon Capture Skid

Figure 4 shows that the acidification cell has been designed so that the polarity of the cell can be reversed. This reversal is essential to aid in reducing mineral deposits on the electrode that is operating as the cathode. Ions that impart hardness to seawater include calcium (Ca^{+2}) and magnesium (Mg^{+2}) ions, and their total concentration is typically less than 2,000 mg/L. Hardness ions can migrate from the seawater in the IX compartment (Figures 1 and 4) or could be introduced into the cathode compartment by the water feeding the cathode compartment. In previous laboratory studies deionized water was used as the feed water to the cathode compartment, so the only hardness ions entering the cathode compartment were from the IX compartment [11]. However, during these tests it was found that the electrical resistance (voltage divided by amperage) increased from 4.07 Ohms to 6.45 Ohms over 150 minutes of operation. This 58% increase in resistance was an indication that minerals (Ca^{+2} and Mg^{+2}) were depositing on the electrode surface of the cathode. These effects can be reduced by reversing the polarity of the electrodes. The change in polarity causes the minerals (scaling) to disassociate from the electrode surface. This is a common practice in Electrodialysis Reversal (EDR) processes. These processes are used to desalinate brackish ground and surface waters. Figure 4 shows that the flow from the individual electrode compartments to the hydrogen stripper are controlled by solenoid valves (valves C and D) to accommodate the necessary changes in polarity to the cell. The frequency of polarity reversal is a part of these studies.

During these tests different CO_2 extraction technologies were tested to determine the most efficient method of liberating the CO_2 gas from the acidified effluent seawater. Specifically, three different size CO_2 stripper columns and a 2.5 x 8 Liqui-Cel polyethylene hollow fiber membrane contactor were evaluated. The $[CO_2]_T$ content of the acidified effluent seawater was measured by coulometry after contact with the different CO_2 extraction technologies to determine the efficiency of each extraction method.

The hydrogen stripper column processes the water from the cathode compartment of the cell as it liberated H_2 gas. The H_2 gas was measured qualitatively throughout the test series by a standard Honeywell gas analyzer.

A Mastech HY3030EX 0-30 amp, 0-30 volt high-current, high-voltage regulated DC power supply controls the pH of the seawater. NRL's Marine Corrosion Facility supplied two (220 Vac, 40 A) and four (110 Vac, 20 A) to power the skid, and a continuous supply of Key West seawater.

5.0 EXPERIMENTAL

5.1 Carbon Capture Skid Operating Conditions

Table 2 provides the operating flow rate conditions for the acidification cell in these test series. Seawater flows through the IX compartment of the cell at 0.5 gal/min (1900 mL/min) (Figures 1 and 4). The Table shows that at this flow rate the maximum calculated CO_2 available for extraction is 0.004 moles/min (0.0023 moles/L CO_2 (100 mg/L) x 1.89 L/min). The RO flow rate to the electrode compartments is 0.06 gal/min (230 mL/min).

Table 2. Electrochemical Acidification Cell Operating Configuration

Applied Current to Electrochemical Cell	**7 amps**	**30 amps**
Operating Seawater Flow Rate IX Compartment	**0.5 gal/min**	**0.5 gal/min**
CO_2 Concentration Extracted at 100% efficiency (eq 13)	0.0040 moles/min	0.0040 moles/min
CO_2 Concentration Extracted at 92% efficiency (eq 13)	0.0037 moles/min	0.0037 moles/min
Operating RO Flow rate to Electrode Compartments	**0.06 gal/min**	**0.06 gal/min**
H_2 Concentration Extracted at 100% (eq 14)	0.002 moles/min	0.010 moles/min
Calculated Synthetic Fuel for 100% CO_2 and H_2		0.027 gal/day

In these test series a 30 volt, 30 amp DC power supply is used to provide current to the acidification cell. Table 2 provides the operating flow rates and currents that were evaluated in the different test series and the calculated minimum amounts of CO_2 and H_2 extractable at those currents and process efficiencies of 92% and 100%. The Table shows that the maximum calculated extractable CO_2 when the cell is operating at 92% efficiency and 7 amps is 0.0037 moles/min. Thus the theoretical flow rate in mL/min to current ratio is estimated to be 270 mL/amp (equation 12). The available hydrogen at 7 amps is 0.002 moles/min. At these hydrogen concentrations, a mole ratio of 0.5:1 H_2 to CO_2 is inefficient for hydrocarbon production. However, the acidification cell was operated at the lower current to compare quantified relationships established between flow rate, current, seawater pH, and CO_2 production found using the small laboratory scale acidification cell with those found in these test series.

There are two principle reactions that take place in the synthesis of a jet fuel fraction ($C_{11}H_{24}$) from CO_2 and H_2. In equation 14, CO_2 is reduced to CO by the reverse water gas shift reaction. Then CO is converted to a theoretical minimum hydrocarbon chain length of eleven by the Fischer-Tropsch reaction shown in equation 15 [5]. The sum of equations 14 and 15 result in equation 16. Equation 16 shows the mole ratio of H_2 to CO_2 is 3.1 to 1, and laboratory results indicate that this ratio is necessary for efficient hydrocarbon production.

$$11CO_2 + 11H_2 \rightarrow 11CO + 11H_2O \qquad \text{(14) Reverse water gas shift}$$

$$11CO + 23H_2 \rightarrow C_{11}H_{24} + 11H_2O \qquad \text{(15) Fischer Tropsch}$$

$$11CO_2 + 34H_2 \rightarrow C_{11}H_{24} + 22H_2O \qquad \text{(16) Sum of equations 14 and 15}$$

To produce feedstock ratios of 3:1 for future hydrocarbon production the current to the cell has to be increased over 4 times to 30 amps. At this current the hydrogen concentration will increase to 0.01 moles/min (equation 13), and the current to flow rate ratio will be decreased from 270 mL/amp to 63 mL/amp. From equations 14 through 16 and the calculated moles/min of CO_2 and H_2 given in Table 2 when the cell is operating at 30 amps, the maximum amount of synthetic $C_{11}H_{24}$ that could theoretically be produced in this apparatus is 0.03 gallons/day (2×10^{-5} gallons/minute or 4.5 mls/hour).

The electrochemical cell was operated at a recovery of 81%. The term "recovery" is used to define the ratio of product quantity (influent seawater flow rate, Table 2) over the total feed quantity to the cell (influent seawater flow rate and influent deionized flow rate, Table 2) as a percent. A high recovery allows the size of the filtration unit along with the energy requirements for the unit to be minimized. This high recovery is possible due to the RO system and the ability to change the polarity of the electrodes in efforts to reduce scaling on the electrodes from hardness ions.

5.2 Carbon Dioxide and Hydrogen Gas Analysis

A UIC Coulometric system (UIC Inc, Joliet, IL 60436) [12] was used to measure the $[CO_2]_T$ content of the seawater throughout these tests. The $[CO_2]_T$ content of the seawater before acidification was measured to be approximately 100 mg/L.

A Honeywell 7866 digital gas analyzer with a thermal conductivity detector was used to measure the amount of H_2 gas from the stripper column throughout the different tests.

5.3 Seawater pH

The seawater pH was monitored continuously using a standard combination electrode as it exits the CO_2 IX compartment of the cell. The seawater pH changes as a function of current applied to the electrochemical acidification cell.

5.4 SAFETY

Safety is paramount in all field operations. Since hydrogen was produced during these test series, it was constantly diluted with air below its lower flammability and explosive limit.

6.0 RESULTS AND DISCUSSION

The NRL team operated the electrochemical acidification carbon capture skid to evaluate, measure, and optimize the system's performance. This analysis concentrates on the electrochemical acidification cell performance during four separate evaluations (January 22th – 27th, April 25th – 29th, July 11th – 15th, August 28th – Sept 1st) as a function of current, pH, time, polarity reversal, and CO_2 and H_2 production and recovery. In addition, it addresses the overall system performance, sustainability, and operational design. These data provide insight into many of the key technological challenges identified with scaling and transitioning the technology.

6.1 Electrochemical Acidification Cell Performance

Electrochemical acidification cell performance data taken during the four separate evaluations of the system at NRL Key West are summarized in Tables A1-A6 in the Appendix. The Tables provide the measured values of the effluent seawater pH, current, voltage, and resistance as a function of time during a polarity cycle. It is critical to evaluate the performance of both electrodes as they cyclically change between functioning as the cathode and anode. The electrode compartments were defined as Polarity (A) and Polarity (B) and the Table indicates

which compartment was functioning as the cathode during the cycle. During each polarity cycle, the cell was operated at the highest processing flow rate of 0.5 gallons/minute (1900 mL/min) of seawater. Between cycles the electrode compartments were flushed with RO water for a defined period of time. The flush cycle is needed to wash the excess H_2, NaOH, O_2 and H^+ from the electrode compartments before the polarity is reversed.

6.1.1 Seawater pH Profiles as a Function of Applied Cell Current over Time

Figures 5-7 compare the pH profiles of 9 polarity cycles (Tables A1-A5) as a function of time and applied cell current (30, 20, 10 amps). Since the performance of both electrodes must be evaluated as they cyclically change between functioning as the cathode and anode, data were collected for two consecutive polarity cycles before any changes were made in current or length of cycle, with the exception of cycle 9.

In Figure 5 the pH profiles of 4 polarity cycles at the maximum design cell current of 30 amps is compared (Tables A1-A2). The first 2 consecutive cycles lasted 59 minutes each with an 86 second flush period between cycles. The next two consecutive cycles ran for 40 minutes each with a longer flush period of 157 seconds for the second cycle. Figure 5 shows that after approximately 19 minutes have passed in all four cycles, the pH of the effluent seawater dropped below 6.00. This time is a function of the strong acid cation exchange resin volume (215 cm^3) in the electrode compartments (Figure 1) and the amount of applied current. After 25 minutes the pH of the effluent seawater was measured below 3.

When the applied cell current is reduced from 30 amps to 20 amps in Figure 6, it took approximately 25 minutes for the pH of the effluent seawater to drop below 6.00 for three cycles (Tables A3 and A5) and 35 minutes to fall below pH 3. At 10 amps, the time for seawater pH to fall below 6.00 increased to 40 minutes and a seawater pH below 3 was never achieved (Figure 7). The applied cell current of 10 amps is comparable to the theoretically calculated minimum applied current of 7 amps needed in these experiments to lower the seawater pH to less than 6.0 and convert HCO_3^- to H_2CO_3 (equation 12). These Figures show that similar pH profiles are achieved for a defined applied cell current as a function of time. This verifies the performance of both electrodes as they cyclically change between functioning as the cathode and anode. In addition it indicates the packing density of the ion exchange material in the electrode compartments is uniform.

Figure 8 is a side by side comparison of pH profiles when the cell was operating in the same polarity configuration at different applied cell currents of 30, 20, and 10 amps. This graph clearly illustrates that seawater pH is proportional to the applied cell current over time.

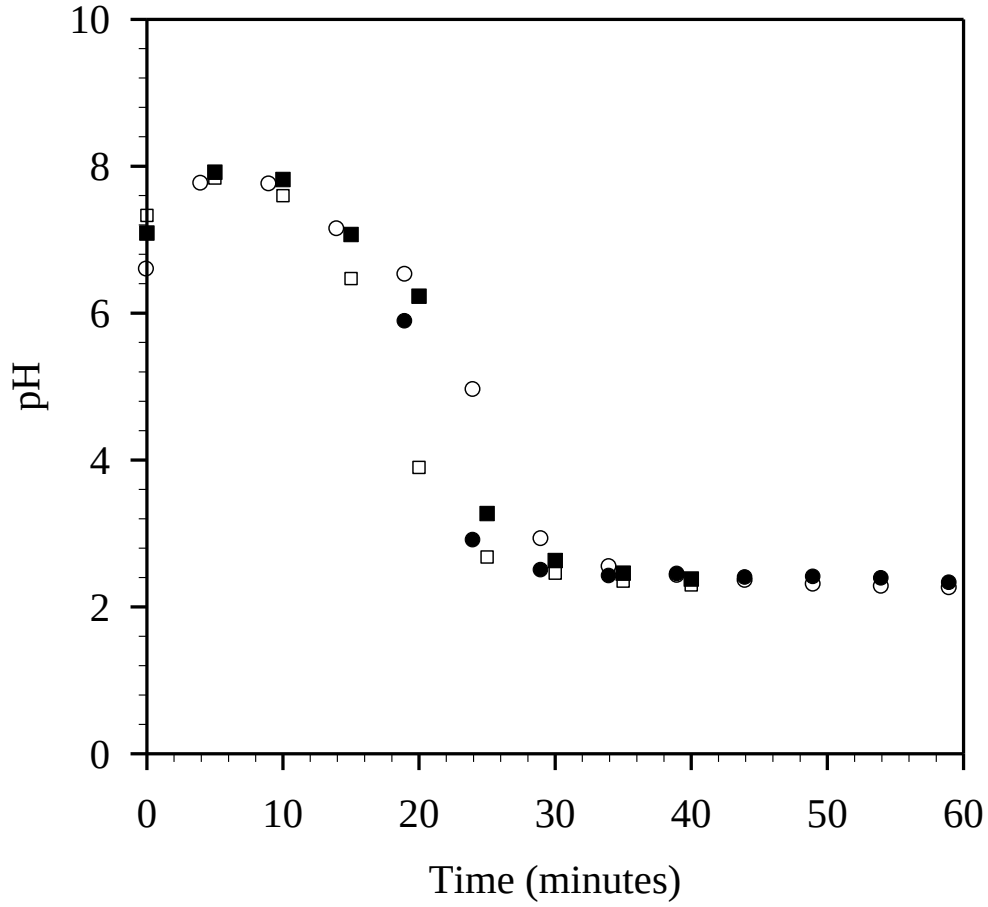

Figure 5. A pH profile comparison of four polarity cycles at 30 amps as a function of time, 59 minute cycle, polarity B (●), 59 minute cycle, polarity A (○), 40 minute cycle, polarity B (■), 40 minute cycle, polarity A (□). Tables A1-A2

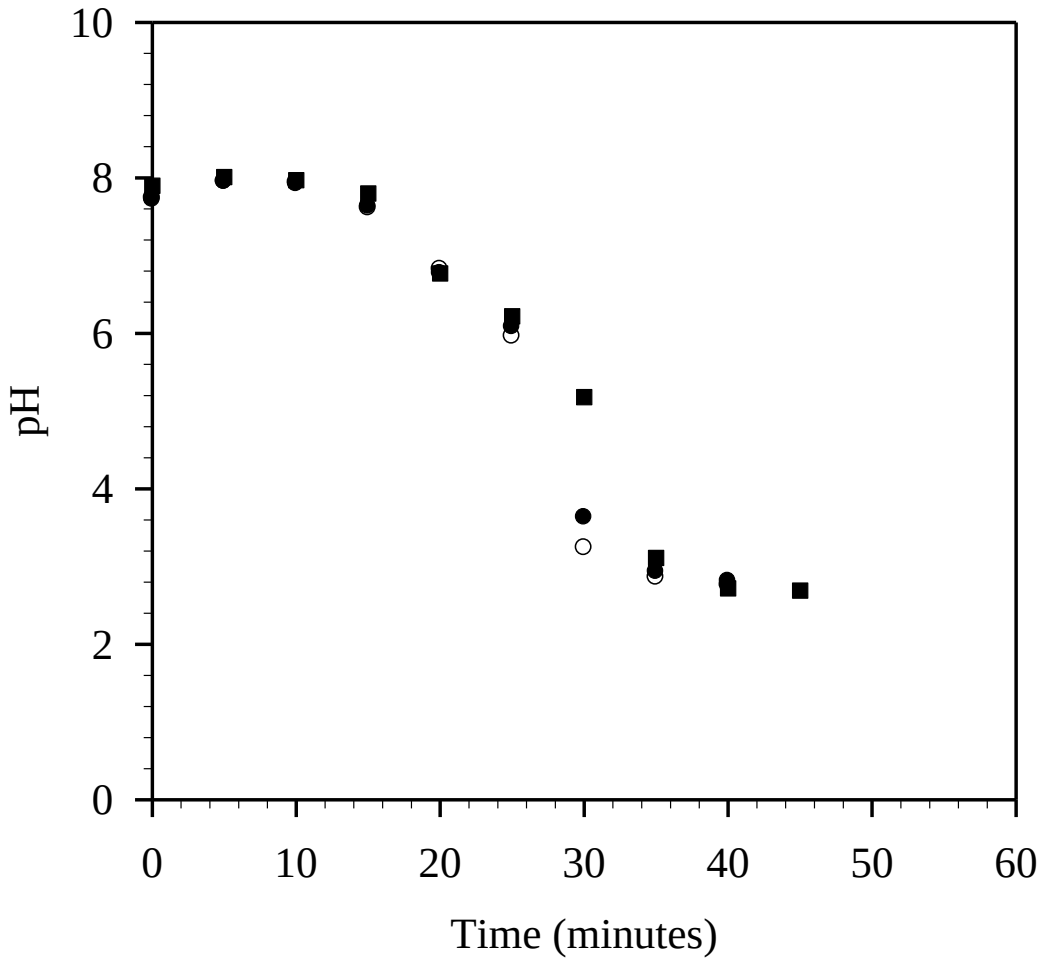

Figure 6. A pH profile comparison of three polarity cycles at 20 amps as a function of time, 40 minute cycle, polarity B (●), 40 minute cycle, polarity B (○), 45 minute cycle, polarity B (■). Tables A3 and A5

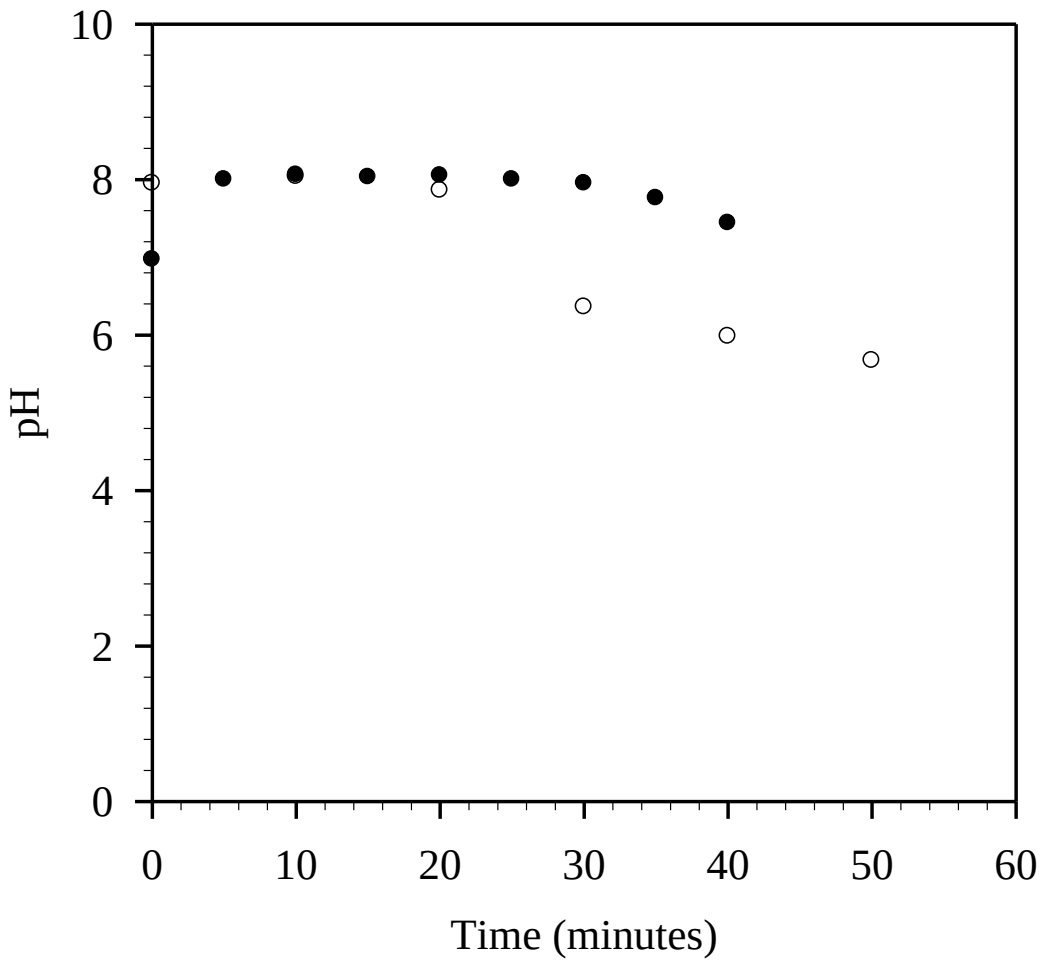

Figure 7. A pH profile comparison of two consecutive polarity cycles at 10 amps as a function of time, 40 minute cycle, polarity B (●) and 40 minute cycle, polarity A (○). Table A4

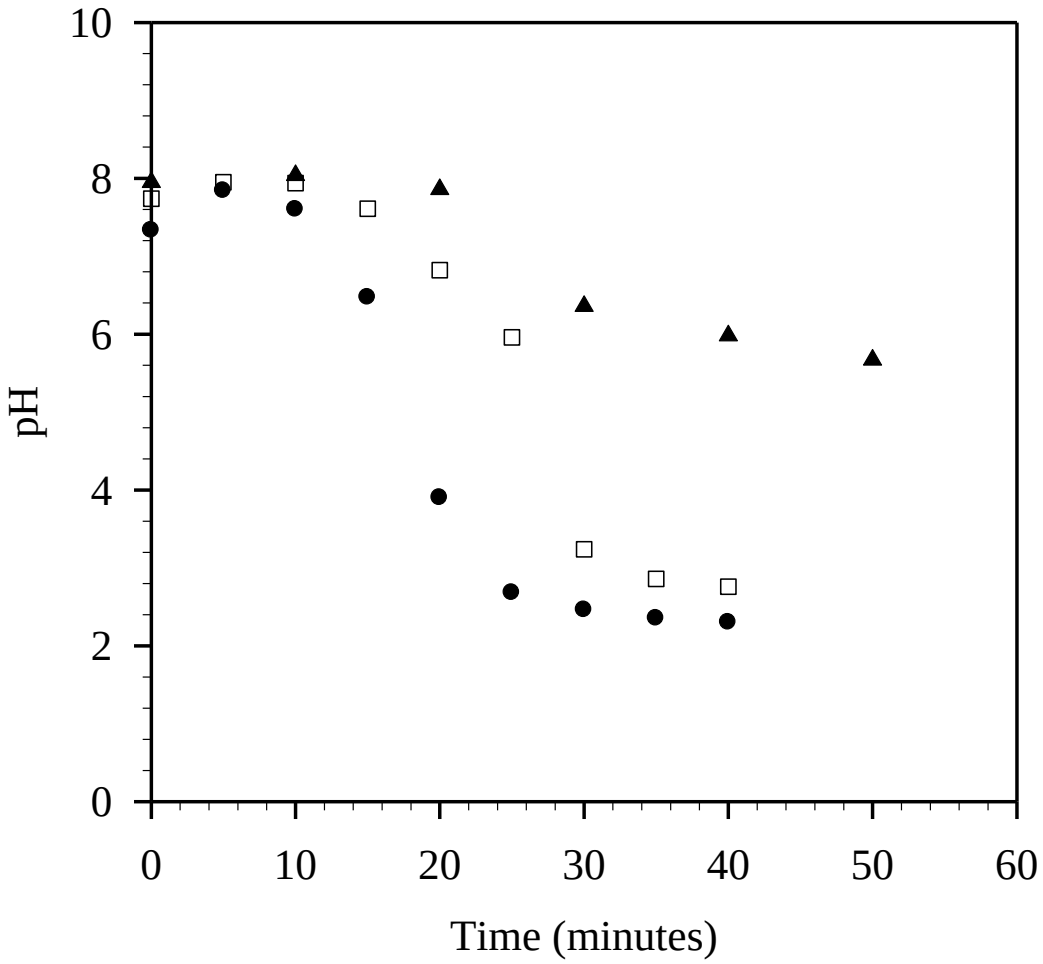

Figure 8. A pH profile comparison for 3 polarity cycles measured at different applied cell currents of, 30 amps 40 minute cycle, polarity B (●), 20 amp 40 minute cycle, polarity B (○), and (▲) 10 amp 45 minute cycle, polarity B. Tables A1-A4

Figures 9 and 10 are the pH profiles for two consecutive polarity cycles at 30 amps and two consecutive cycles at 20 amps. Each cycle was 40 minutes long before the polarity was switched and the electrode compartments were flushed. While Figures 5-7 were side by side comparisons of 2 consecutive cycles as a function of time and applied current, these Figures illustrate the 30 amp and 20 amp consecutive cycles along with the flush cycle in succession. The Figures clearly illustrate that once a cycle ends, the electrode compartments are flushed, the polarity is switched, and a new cycle begins, the pH of the effluent returns to that of the influent. This is critical because equilibrium conditions of the cation exchange material in the cell's electrode compartments must be re-established upon changing the polarity of the cell. When the polarity of the cell is reversed, the H^+ ions generated on the electrode now functioning as the anode exchange on the resin and release Na^+ ions. The Na^+ ions then migrate through the cation exchange membrane and into the IX compartment. The migrating Na^+ ions pass through the cation exchange membrane at the electrode now acting as the cathode and exchange on the resin to convert all the resin in that compartment to the sodium form. Equilibrium conditions are re-

established during the polarity cycle when all the resin in the compartment now acting as the anode is regenerated back into the hydrogen form and all the resin in the cathode is regenerated back into the sodium form. Figure 9 shows that at 19 minutes and 30 amps, the ion exchange material in the electrode compartments reach equilibrium or a level of regeneration, allowing more H^+ ions to pass through the membrane closest to the anode to acidify the seawater. This time is increased to 25 minutes as the applied cell current is reduced to 20 amps as shown in Figure 10. These characteristics are specific to the IONPURE cell used in this evaluation. As a result the pH of the effluent seawater drops. Since the amount of H^+ ions generated from the oxidation of water on the electrode functioning as the anode is proportional to the applied electrical current, the more current applied to the cell, the faster the cell will reach a state of equilibrium.

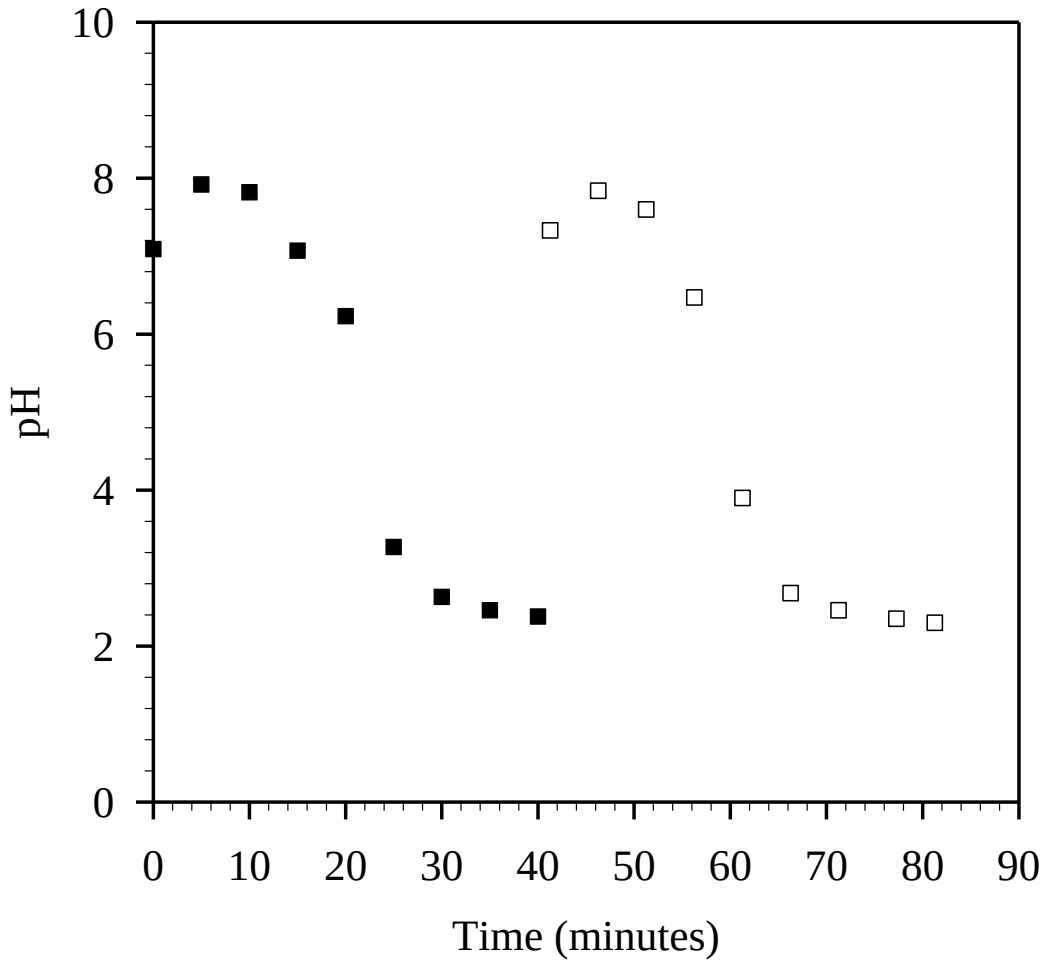

Figure 9. A pH profile in succession of two consecutive 40 minute polarity cycles at 30 amps as a function of time, 40 minute cycle, polarity B (■) and 40 minute cycle, polarity A (□). Table A2

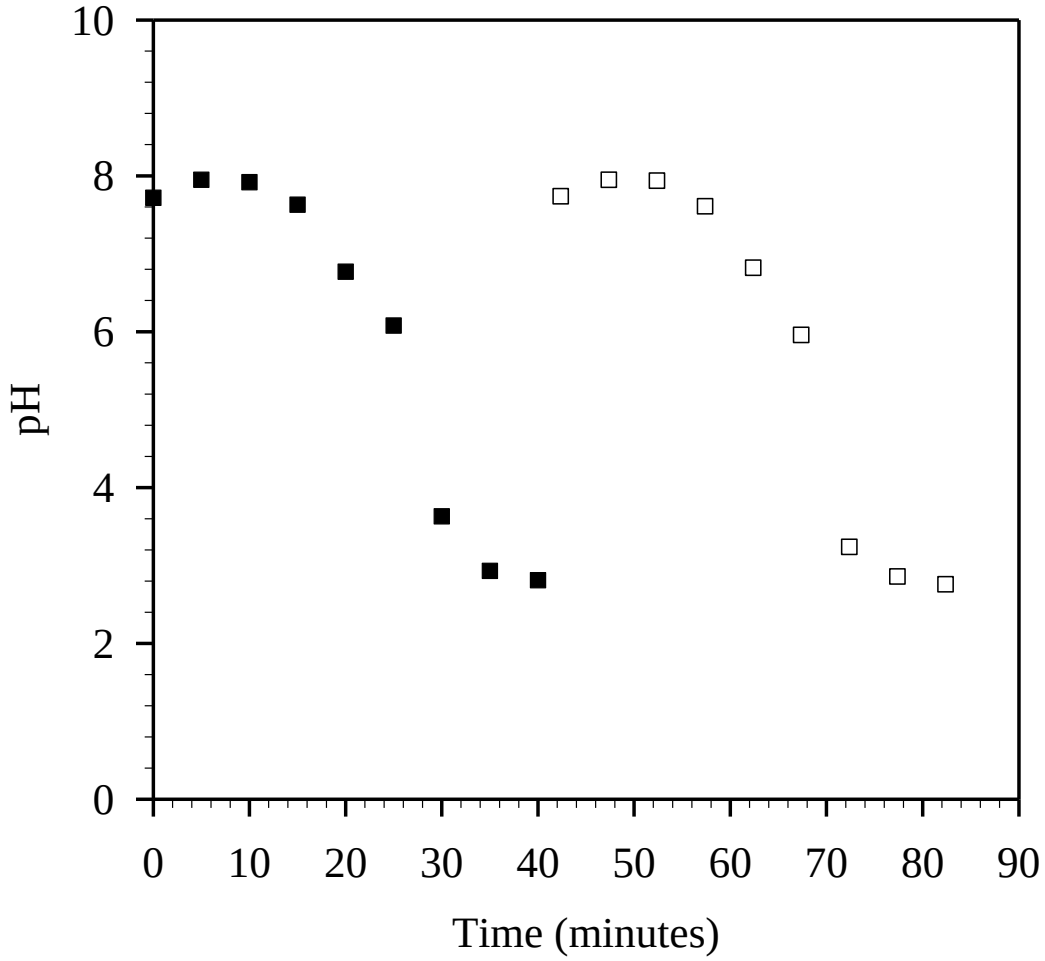

Figure 10. A pH profile in succession of two consecutive 40 minute polarity cycles at 20 amps as a function of time, 40 minute cycle, polarity B (■), and 40 minute cycle, polarity A (□) Table A3

These data provide important insight into the future design of the cell. The equilibrium times may be reduced by changing the electrode compartment configuration and reducing or eliminating the ion exchange material. Eliminating the ion exchange material will require relying solely on the ion exchange properties of the membrane in the compartment. Design efforts can also be directed toward maintaining a constant effluent seawater pH throughout the consecutive polarity cycles.

6.1.2 Electrical Resistance as a Function of Time and Applied Cell Current

An increase in electrical resistance as a function of time is a sign of hardness scaling on the cathode. Scaling (mineral deposits) takes place at the high-pH surface of the cathode. The formation of mineral deposits decreases the electrode surface area causing an increase in the electrical resistance of the entire cell. This in turn leads to a reduction in current efficiencies

and could cause a pressure drop in the electrode compartment functioning as the cathode. By cyclically reversing the polarity of the cell's electrodes, the mineral deposits will be reduced on the electrode that was operating as the cathode in the previous cycle. The change in polarity causes the minerals (scaling) to disassociate from the electrode surface. Evaluation of how well polarity reversal of the cell minimized mineral deposits on the electrode functioning as the cathode was one of the key objectives of these tests.

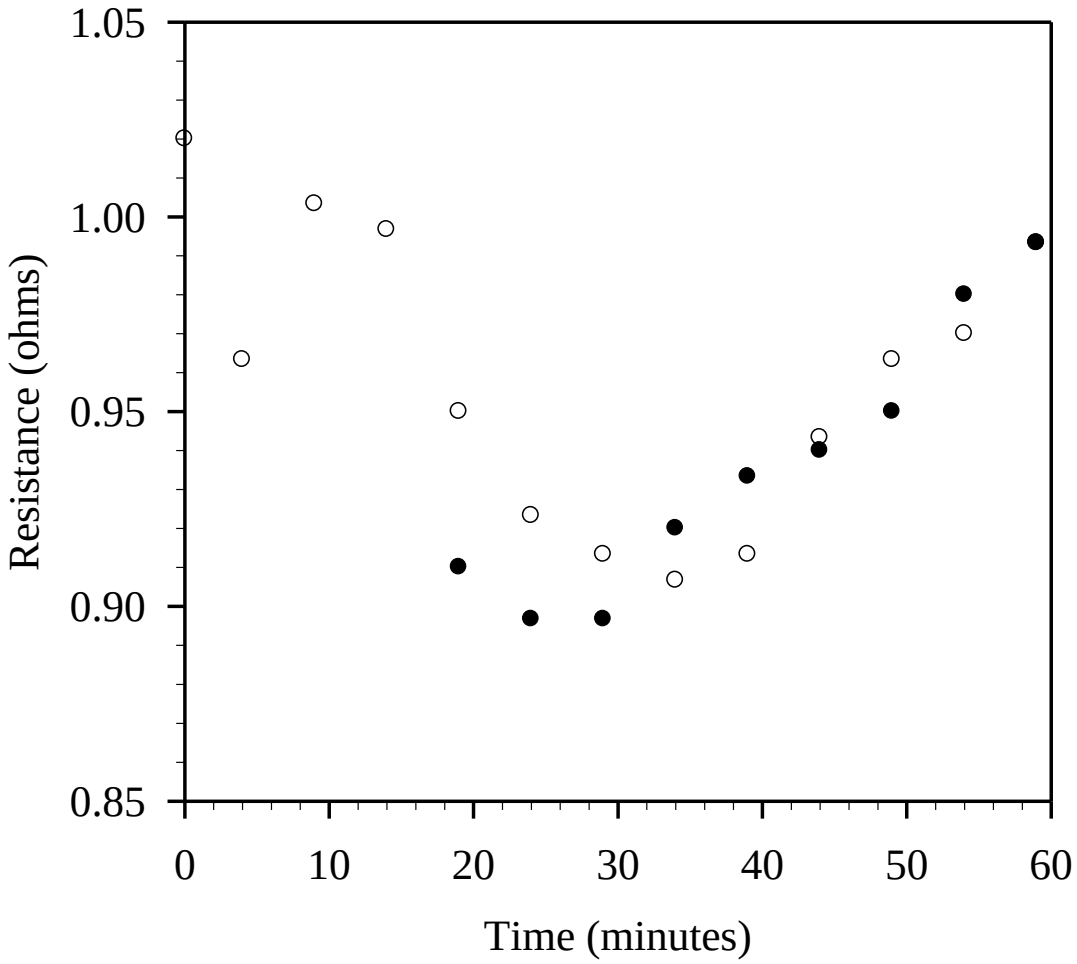

Figure 11. The electrical resistance comparison of two consecutive 59 minute polarity cycles at 30 amps as a function of time, polarity B (●) and polarity A (○). Table A1

Figure 11 is a plot of electrical resistance (voltage divided by amperage) as a function of time for the two 59 minute consecutive polarity cycles at 30 amps. Comparing both cycles shows that the resistance decreases by approximately 11% over the first 29 minutes of operation. During the remaining 30 minutes of both cycles the resistance increases by 10 to 11%.

Figure 12 illustrates the 40 minute consecutive polarity cycles at 30 amps in succession. During each cycle the electrical resistance decreases by approximately 10 to 11% in the first 25 minutes and then increases to 0.91 ohms over the remaining 15 minutes. Figure 12 also shows that once

the electrode compartments are flushed for 86 seconds and the polarity is reversed, the electrical resistance of the cell at the start of the fourth cycle was as high as 1.0 ohms. This is explained by the conductivity of the ion exchange resin in the electrode compartments upon polarity reversal. When the polarity is reversed, the ion exchange resin in the electrode compartment functioning as the anode is in the sodium form. This form of the resin is less conductive and as a result more voltage to the cell is needed to maintain the current. The voltage is reduced as equilibrium conditions in the cell are re-established. At the same time minerals are dissociated from the electrode that is operating as the cathode in the previous cycle.

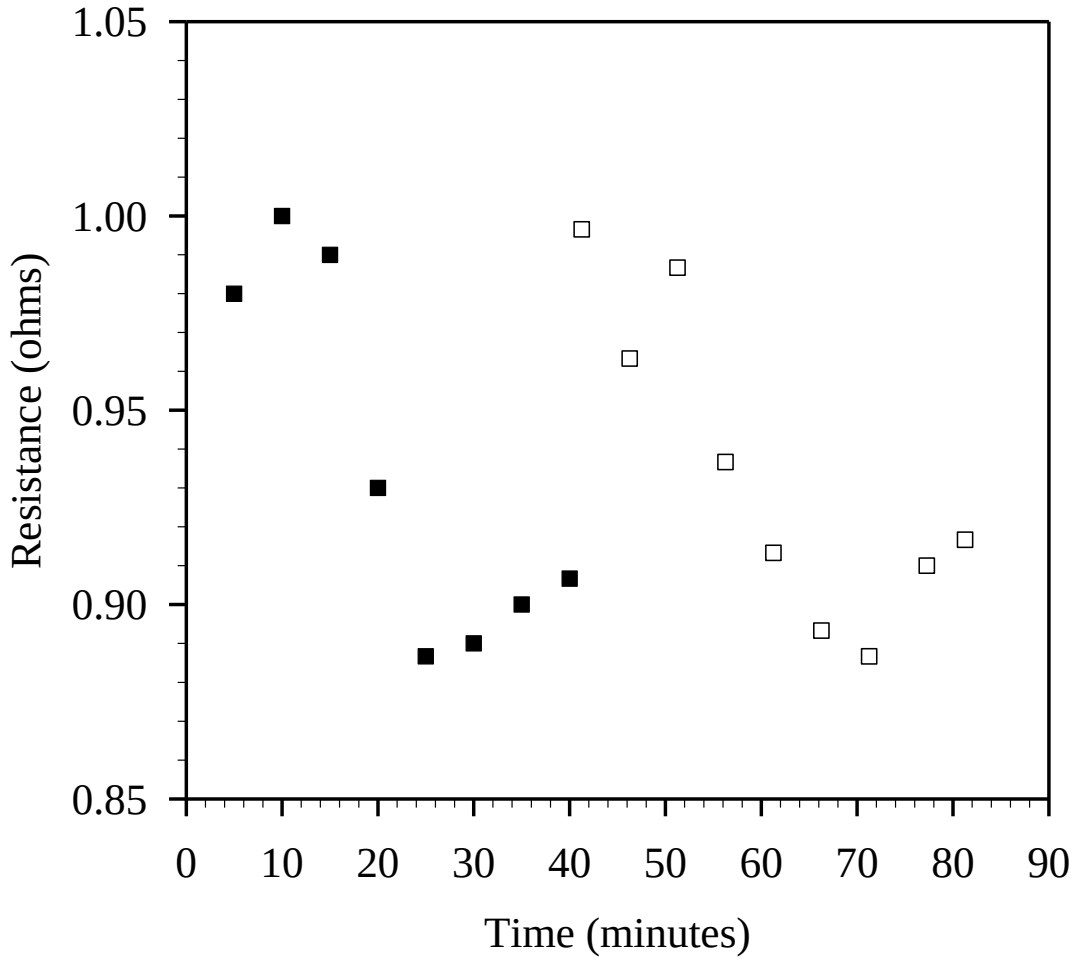

Figure 12. The electrical resistance in succession of two consecutive 40 minute polarity cycles at 30 amps as a function of time, polarity B (■) and polarity A (□). Table A2

Figure 13 shows the measured resistance of the cell when the applied current was reduced from 30 amps to 20 amps. The Figure indicates that the resistance of the cell did not decrease until approximately 20 minutes into the cycle. This phenomenon is also attributed to the equilibrium conditions in the cell. At lower applied cell current, less H^+ ions are produced at the anode, therefore it takes longer for equilibrium conditions of the cation exchange material to re-establish in both electrode compartments. It appears that after 35 to 40 minutes the resistance of the cell

begins to increase. However, during these experiments the polarity cycles were not long enough at this applied cell current to completely establish the time in which hardness and scaling on the cathode occurred.

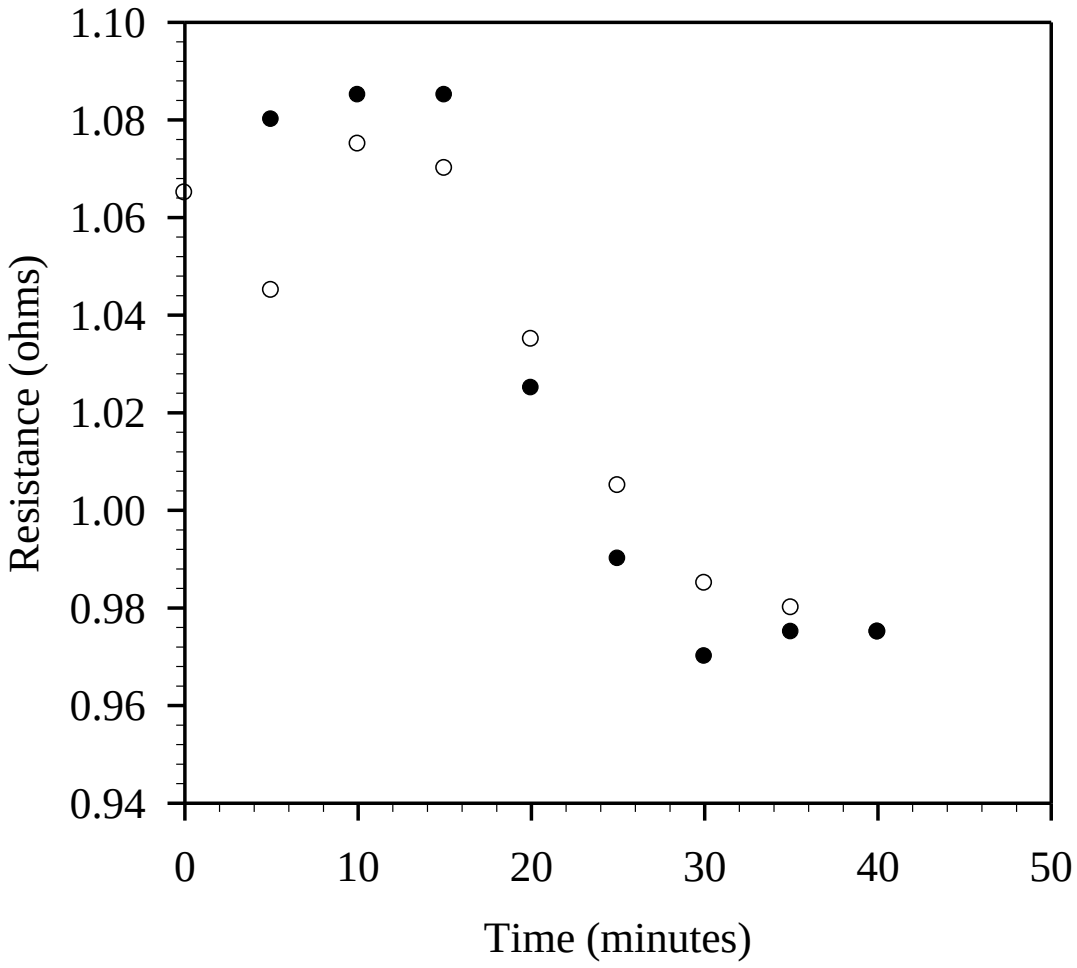

Figure 13. The electrical resistance in succession of two consecutive 40 minute polarity cycles at 20 amps as a function of time, polarity B (●) and polarity A (○). Table A3.

From the electrical resistance data at the higher applied cell current of 30 amps (Figures 11 and 12), an empirical factor of 900 amp-min was ascertained by multiplying the applied current by the time in which signs of hardness and scaling on the cathode were observed at that applied current (30 amps x 30 minutes = 900 amp-min). This factor is specific to the IONPURE cell and can be used to calculate operating time guidelines for the cell at any applied current as shown in equation 17 and listed in Table 3.

$$\text{Operational Time, min} = (900 \text{ amp-min})/(\text{Applied Current, amp}) \quad (17)$$

Table 3. Electrochemical Acidification Cell Theoretical Operating Parameters

Applied Current (Amps)	**Operational Time (min)**	**Calculated H_2 Generation Cathode (mL/min)**	**Calculated CO_2 Generation (mL/min)**
2	450	14	28
4	225	28	55
6	150	42	83
8	113	55	83
10	90	69	83
12	75	83	83
14	64	97	83
16	56	111	83
18	50	125	83
20	45	138	83
22	41	152	83
24	38	166	83
26	35	180	83
28	32	194	83
30	30	208	83

The data in Figures 5-13 suggest that the theoretical operational times in Table 3 for an applied cell current are realistic. They also suggest that the pH profile during these operational times may be improved by future system and cell design changes. These changes include altering the electrode compartment configuration by reducing or eliminating the ion exchange material in the compartment. This could result in faster equilibrium conditions upon polarity reversal and improved current efficiencies.

6.1.3 Cell Performance after Prolonged Shutdown Period

The NRL team operated the electrochemical acidification carbon capture skid on four separate occasions. In January 2011 the system's design and performance were initially evaluated. After this test series and the subsequent test series that followed, power was removed from the skid and its components were rinsed and flushed with fresh water (Figure 2 and 4). The skid was covered in a tarp and left un-operational. When activity was recommenced during each test series, the system performance was verified by measuring the seawater pH and cell voltage as a function of time. Figure 14 compares the pH profiles measured as a function of time during the each different test series. At an applied cell current of 20 amps the pH profiles for each test series were similar.

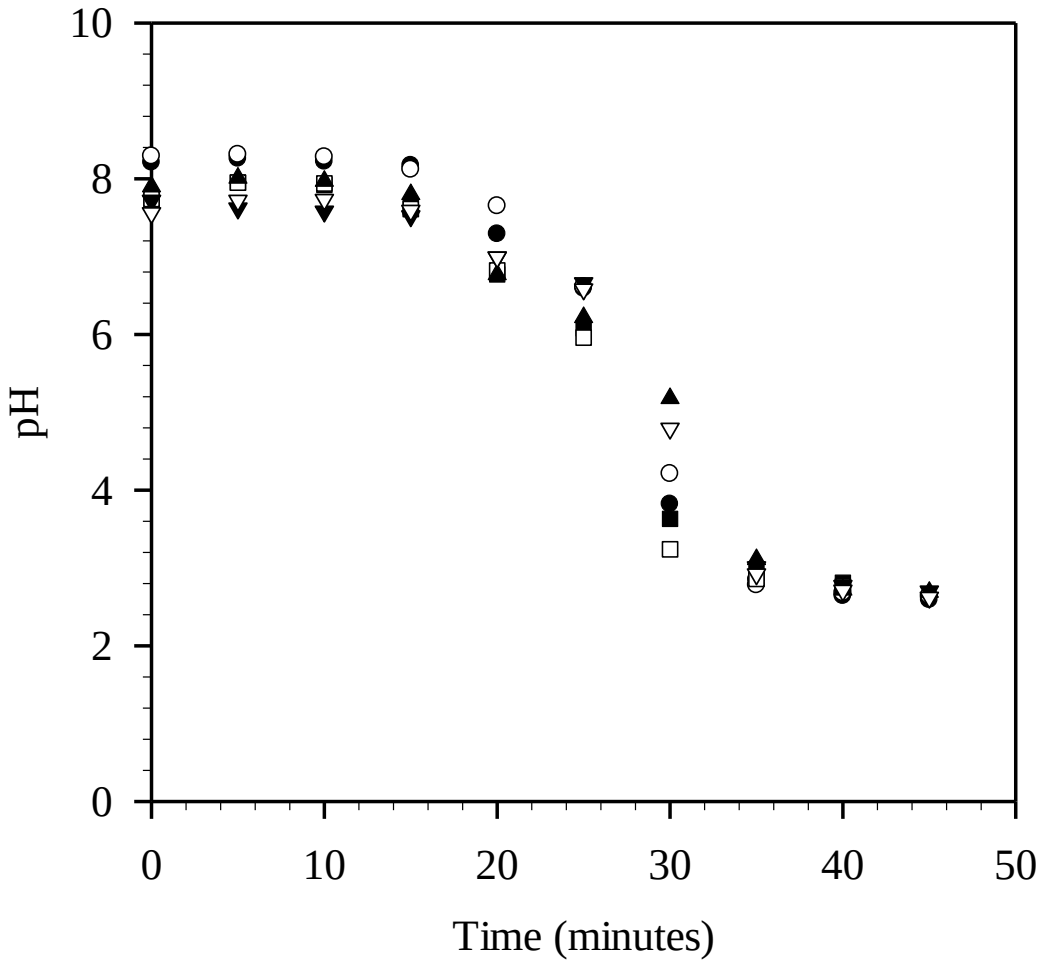

Figure 14: A pH profile comparison of five polarity cycles at 20 amps as a function of time, 45 minute cycle, polarity A (●), 45 minute cycle, polarity B (○), 40 minute cycle, polarity B, (■) 40 minute cycle, polarity A (□), 45 minute cycle, polarity B(▲), 45 minute cycle, polarity A (▼), 45 minute cycle, polarity B (∇). Tables A3-A7

Figure 15 compares the electrical resistance profiles at 20 amps of applied cell current for both test series. The graph shows that while the resistance in the cell varies between the test series, the overall resistance profiles and re-equilibration times remain consistent. The difference in measured electrical resistance between the test series may be attributed to the bulk temperature of the influent seawater and its overall composition. In general, the electrical resistance in the cell is strongly affected by temperature. A standard IONPURE module's resistance will change by approximately 2% per 1 degree Celsius change in water temperature. As water temperature increases, the electrical resistance in the cell decreases. The average seawater temperature in January, April, July, and August was 22 ^{o}C, 26 ^{o}C, 30 ^{o}C,, and 31 ^{o}C. The salinity of seawater also changes with temperature. At higher seawater temperatures the electrical conductivity of the seawater increases as the salinity increases due to the evaporation process of surface waters. This will lead to a decrease in the electrical resistance within the cell.

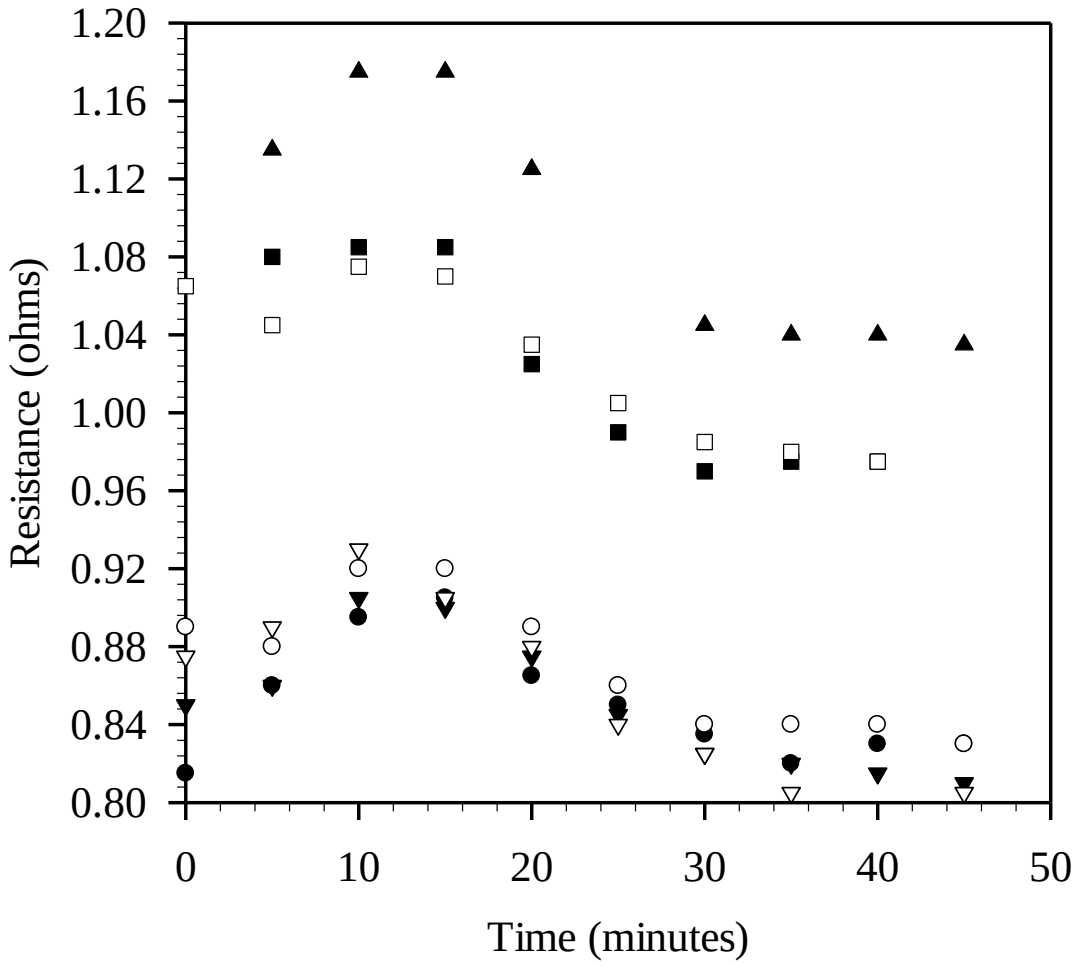

Figure 15: A electrical resistance profile comparison of five polarity cycles at 20 amps as a function of time, 45 minute cycle, polarity A (●), 45 minute cycle, polarity B (○), 40 minute cycle, polarity B, (■) 40 minute cycle, polarity A (□), 45 minute cycle, polarity B(▲),45 minute cycle, polarity A (▼), 45 minute cycle, polarity B (▽). Tables A3-A7

The pH profiles and electrical resistance results for each test series are significant because they indicate that the materials in the cell (ion exchange resin, inert beads, ionic change membrane) maintained their integrity and did not fail as a result of prolong stagnation and inactivity between test evaluations in a warm tropical climate. In such climate, biological growth and contamination could result in diminished cell performance. Indeed when the system was restored to operation in April, the team experienced the smell of hydrogen sulfide coming from the water produced by the RO system. The team is attributing this to microbiological activity from residual seawater in the RO unit and filter housings. Since this evaluation, careful consideration was made to ensure no residual seawater was left in any part of the system while it was not operational, and as a result hydrogen sulfide was never smelled again upon restored operation of the system in July and August.

6.2 Carbon Capture Analysis

NRL laboratory studies have shown that carbon dioxide is readily removed from seawater at a pH less than 6.0. The studies also suggest that at high seawater flow rates, assisted degassing by vacuum is required and sample volume and applied vacuum conditions are important parameters. During the first electrochemical acidification carbon capture skid test series in January of 2011, effluent seawater samples were collected during a 20 amp 40 minute polarity cycle to measure their pH and $[CO_2]_T$. Figure 16 illustrates percent removal of $[CO_2]_T$ plotted as a function of pH. It is important to note that these samples were taken before the effluent seawater reached the carbon dioxide stripper column. Thus the Figure indicates that approximately 50% of the CO_2 was spontaneously degassed from the effluent seawater below pH 4. At the stripper column the samples were degassed by a 600 mL/min vacuum pump operating at a vacuum of 12 inches of Hg. The ability of the vacuum pump to degas the effluent seawater further than 50% could not be assessed during this evaluation because it was found that the system developed a leak in the tubing used to construct the line.

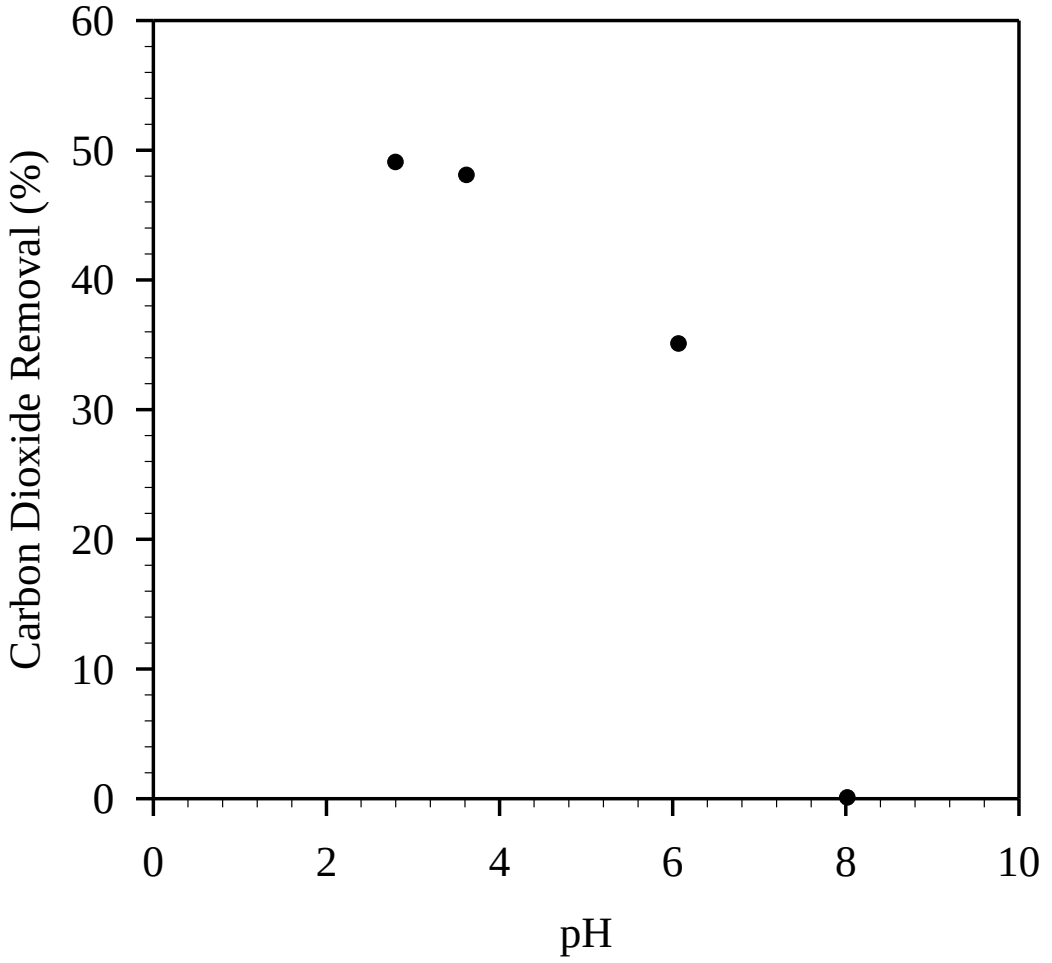

Figure 16. Carbon dioxide removal as a function of pH for effluent seawater samples taken during a 40 minute polarity cycle at 20 amps, before the gas stripper column.

During the April 2011 evaluation of the system at NRL-Key West the tubing was replaced so that an adequate seal would provide the vacuum necessary to degas the effluent seawater further than what was obtainable by just acidifying the seawater as shown in Figure 16. However, after an adequate seal was obtained, there was no measurable improvement in the recovery of CO_2 from the seawater at pH less than 6.

Two additional CO_2 stripper columns were constructed and tested in efforts to improve CO_2 recovery. These stripper columns were larger in diameter and filled with more packing material in efforts to increase the seawater surface area during vacuum degassing. Throughout testing of these columns no measurable improvements in CO_2 recovery were observed over the original stripper column design.

Gas permeable membranes are available commercially for the removal or addition of gases from liquids. Most of these applications are near atmospheric pressure and include water purification, blood oxygenation and artificial lung devices [13-16] However some are operated at higher pressures such as beverage carbonation [17,18]. It is well known that these membranes work on the principle of dissolved gases such as carbon dioxide diffusing across the membrane through the pores as a function of differential partial gas pressures. Therefore a Liqui-Cel polyethylene hollow fiber membrane contactor was tested as another method to increase seawater surface area and thus increase CO_2 recovery from seawater at pH below 6. In these experiments, approximately 30 inches of Hg vacuum was applied by a rotary vane vacuum pump to the inside of the hollow fiber membrane tubes in the contactor, as effluent seawater passed over the outside of the membrane fibers at a flow rate of 0.5 gallons/minute.

Figure 17 shows the percent removal of $[CO_2]_T$ plotted as a function of effluent seawater pH for two consecutive 45 minute polarity cycles at 20 amps of applied current. From the Figure it is clear that 92% of the CO_2 was removed from the effluent seawater at pH 4 at ~ 30 inches of Hg vacuum. As the effluent seawater pH was lowered further to 2.6 no measureable increase in CO_2 removal was observed. These results indicate that a viable technology has been identified and demonstrated for CO_2 recovery on the carbon capture skid.

Since the CO_2 recovered is contaminated by the oil in the rotary vane pump, the next step in the process is to purchase and test a gear pump or diaphragm pump that is capable of 25 to 30 inches of Hg. Under high vacuum, there is always a chance for the water to permeate through the membrane and be pulled into the pump. A gear pump or a diaphragm pump will allow any water or water vapor to enter the pump without damaging the pump. In addition, the CO_2 gas can be collected and concentrated from the effluent seawater and sent to the thermal conductivity detector for analysis.

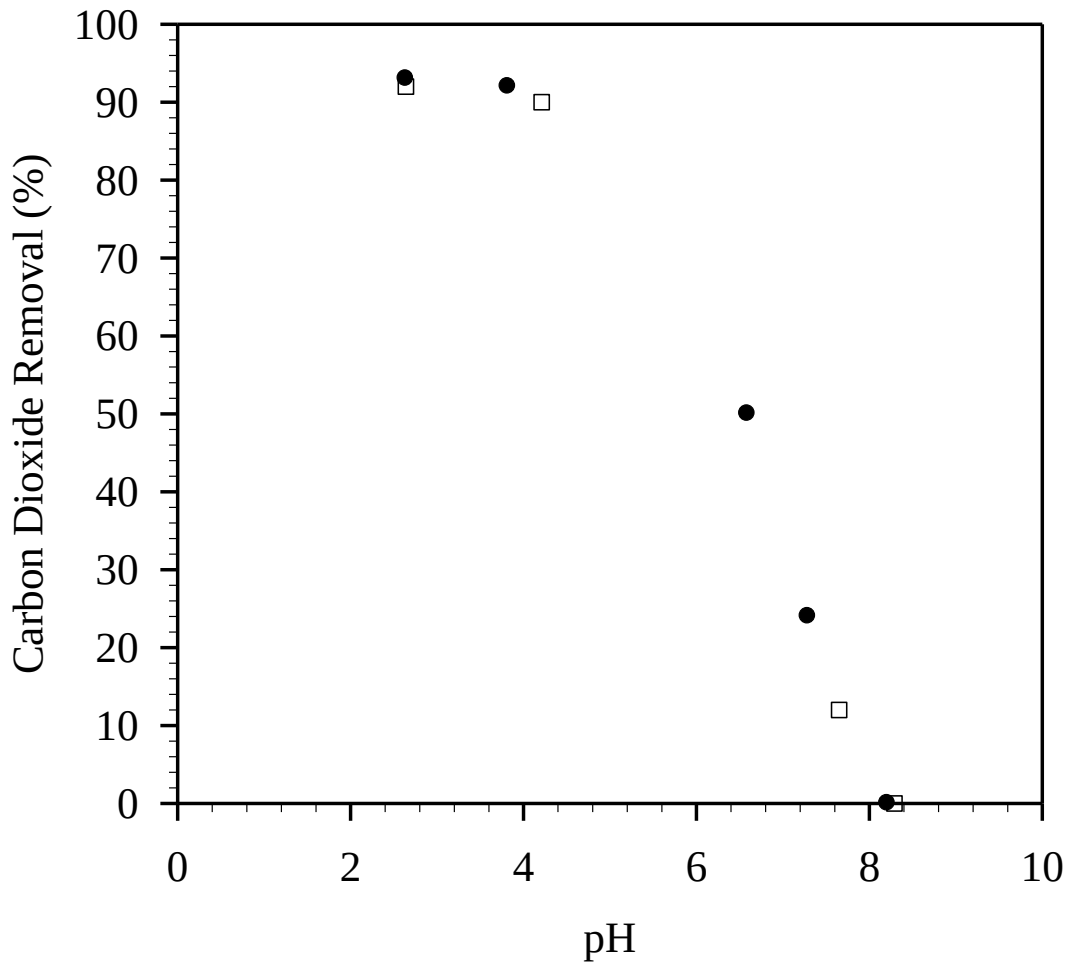

Figure 17. Carbon dioxide removal as a function of pH for effluent seawater samples taken during two consecutive 45 minute polarity cycles at 20 amps, after contact with hollow fiber membrane contactor.

When the vacuum applied to the contactor was decreased from approximately 30 inches of Hg to 26.95 inches of Hg using a diaphragm pump, CO_2 recovery was reduced from 92% to 67% (Figure 18). This 27% loss in CO_2 recovery from the acidified seawater using membrane contactors clearly indicates the rate and amount of CO_2 removal is vacuum dependent.

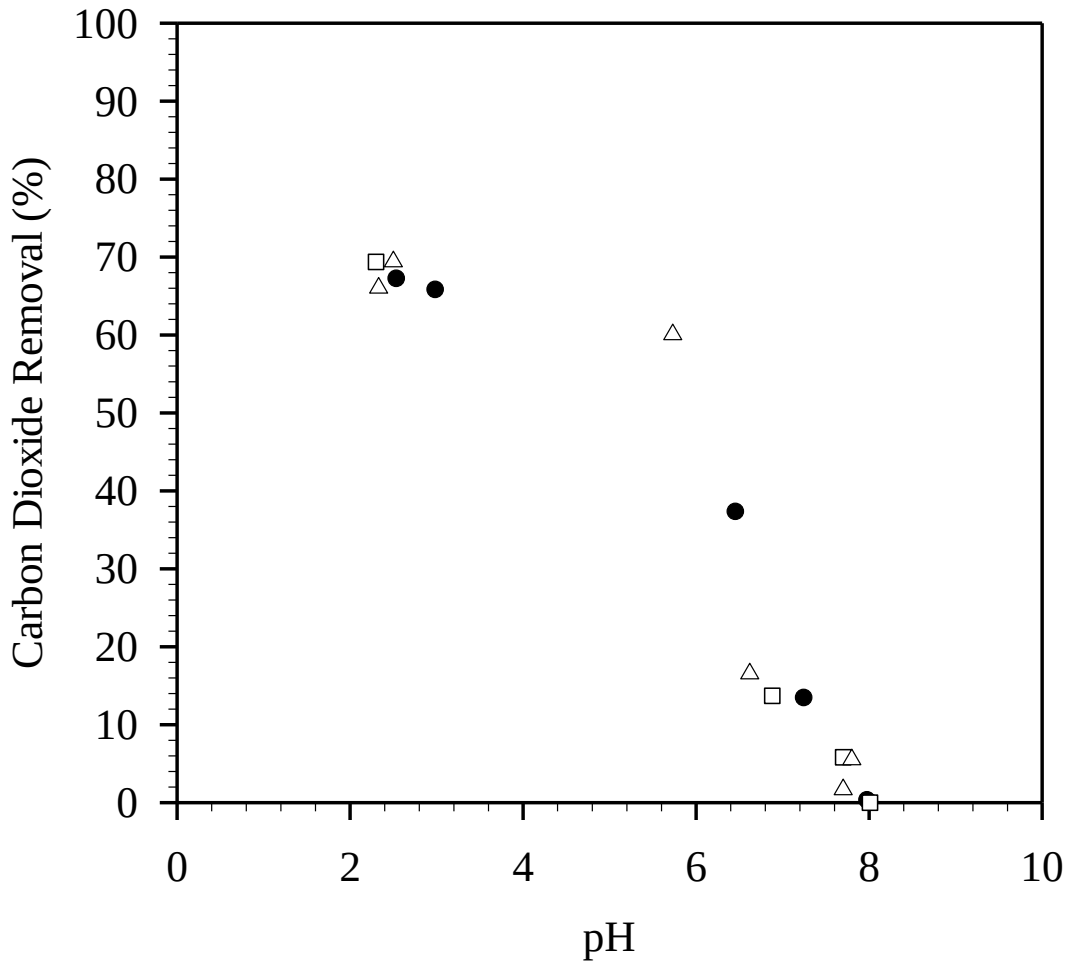

Figure 18. Carbon dioxide removal as a function of pH for effluent seawater samples taken from the electrochemical acidification cell during three 30 minute polarity cycles at 30 amps after contact with hollow fiber membrane contactor at seawater flow rate of 0.5 gal/minute and vacuum conditions ~ 26.95 inches of Hg.

7.0 CONCLUSIONS

In conclusion, four separate evaluations of the electrochemical acidification cell performance have shown that the cell was successfully scaled-up, incorporated into a mobile platform, and operated successfully. The pH profiles from four separate evaluations verify that the acidification cell reduces the seawater pH below 6.00 as reproducibly as intended. The electrical resistance profiles show that cyclically reversing the polarity of the cell's electrodes minimizes the effects of scaling (mineral and organic deposits). In addition, the operational times were

ascertained in order to provide operational parameters for the cell. From the pH profiles and the operational parameters, new cell design parameters are being developed to establish faster equilibrium conditions in the cell upon polarity reversal and improvements in current efficiencies.

Finally, quantitative measurements indicate that 92% of the $[CO_2]_T$ is removed from the effluent acidified seawater after contact with the hollow fiber membrane contactor under higher vacuum conditions (30 inches of Hg) and seawater pH $\leq$ 4. This 42% increase in CO_2 recovery is significant because the initial studies in Key West showed that recovery of 50% could be achieved by spontaneous natural degassing. In addition the results indicate the rate and amount of CO_2 removal is vacuum dependent.

8.0 MILESTONES

- Successful demonstration of system component sustainability process efficiency and continuous production of hydrogen and carbon dioxide using the electrochemical acidification carbon capture skid were achieved during four separate test evaluations of the skid.

- Successful recovery of CO_2 from effluent seawater (92%) at seawater effluent pH $\leq$ 4 using the membrane contactor.

- Successfully recovery of H_2 using standard gas stripper column.

- Successful reproducibility of pH profile and electrical resistance trends between four separate evaluations of the system.

- External filtration system was added to maintain the systems operational capacity by ensuring proper filtration for the cell, the RO system, and the contactor to ensure future continuous long term operation.

9.0 RECOMMENDATIONS FOR FUTURE STUDIES

After these initial evaluations the following studies are recommended:

- Pursue design modifications to the commercial backup cell by changing the amount and type of strong acid cation exchange resin.

- Test the modifications made to the cell in the current skid design.

- Determine minimum vacuum requirements necessary for extraction of CO_2 using the hollow fiber membrane contactor.

- Concentrate CO_2 gas from the membrane contactor and obtain quantitative measurements using a thermal conductivity detector.

- Test spray tower technology for extraction efficiency of CO_2 from the acidified seawater.

10.0 REFERENCES

[1] "Single Naval Fuel at Sea Feasibility Study – Phase One" NAVAIRSYSCOM Report 445/02-004, October 25, 2002.

[2] Davis, B. H. Topics in *Catalysis* **2005**, *32*, 143-168.

[3] Hardy, D. R. Zagrobelny, M.; Willauer, H. D.; Williams, F. W. *Extraction of Carbon Dioxide From Seawater by Ion Exchange Resin Part I: Using a Strong Acid Cation Exchange Resin*; Memorandum Report 6180-07-9044; Naval Research Laboratory: Washington DC, 20 April 2007.

[4] Willauer, H. D.; Hardy, D. R.; Lewis, M. K.; Ndubizu, E. C.; Williams, F. W. Recovery of CO_2 from Aqueous Bicarbonate Using a Gas Permeable Membrane. *Energy & Fuels*, **2009**, *23*, 1770- 1774.

[5] Willauer, H. D.; Hardy, D. R.; Lewis, M. K.; Ndubizu, E. C.; Williams, F. W. "Recovery of $[CO_2]_T$ from Aqueous Bicarbonate Using a Gas Permeable Membrane" Memorandum Report 6180-08-9129; Naval Research Laboratory: Washington DC, 25 June 2008.

[6] Willauer, H. D.; Hardy, D. R.; Lewis, M. K.; Ndubizu, E. C.; Williams, F. W. "Extraction of CO_2 From Seawater By Ion Exchange Resin Part II: Using a Strong Base Anion Exchange Resins" Memorandum Report 6180-09-9211; Naval Research Laboratory: Washington DC, 29 September 2009.

[7] Dorner, R. W.; Hardy, D. R.; Williams, F. W.; Davis, B. H.; Willauer, H. D. Influence of Gas Feed Composition and Pressure on the Catalytic Conversion of CO_2 Using a Traditional Cobalt-Based Fischer-Tropsch Catalyst. *Energy & Fuels*, **2009**, 23, 4190-4195.

[8] Dorner, R. W.; Willauer, H. D.; Hardy, D. R.; Williams, F. W. "Effects of Loading and Doping on Iron-based CO_2 Hydrogenation Catalyst," Memorandum Report 6180-09-9200; Naval Research Laboratory: Washington DC, 24 August 2009.

[9] Dorner, R. W.; Hardy, D. R.; Williams, F. W.; Davis, B. H.; Willauer, H. D. K and Mn doped Iron-based CO_2 Hydrogenation Catalysts: Detection of $KAlH_4$ as part of the catalyst's active phase. *Applied Catalysis*, **2010**, 373, 112-121.

[10] Willauer, H. D.; Hardy, D. R.; Lewis, M. K.; Ndubizu, E. C.; Williams, F. W. The Effects of Pressure on the Recovery of CO_2 by Phase Transition from a Seawater System by Means of Multi-layer Gas Permeable Membranes. *J. Phys. Chem. A*, **2010**,114, 4003-4008.

[11] DiMascio, F.; Willauer, H. D.; Hardy, D. R.; Lewis, M. K.; Williams, F. W. "Extraction of Carbon Dioxide From Seawater By An Electrochemical Acidification Cell Part I. Initial Feasibility Studies," Memorandum Report 6180-10-9274; Naval Research Laboratory: Washington DC, 23 July 2010.

[12] Johnson, K. M., King, A. E., Sieburth, J. Coulometric TCO_2 Analyses for Marine Studies: An Introduction. *Marine Chem.* **1985**, *16*, 61.

[13] Bhaumik, D.; Majumdar, S.; Fan, Q.; Sirkar, K. K. Hollow Fiber Membrane Degassing in Ultrapure Water and Microbiocontamination. *J. Membr. Sci*. **2004**, *235*, 31.

[14] Lund, L. W.; Hattler, B. G.; Federspiel, W. J. Gas Permeance Measurement of Hollow Fiber Membranes in Gas-Liquid Environment. *AIChE J.* **2002**, *48*, 635.

[15] Lund L. W.; Federspiel, W. J.; Hattler, B. G. Gas Permeability of Hollow Fiber Membranes in a Gas-Liquid System. *J. Membr. Sci*. **1996**, *117*, 207.

[16] Eash, H. J.; Jones, H. M.; Hattler, B. G.; Federspiel, W. J. Evaluation of Plasma Resistant Hollow Fiber Membranes for Artificial Lungs. *ASAIO J.* **2004**, *50*, 491.

[17] Bosko, R. S. Hollow Fiber Carbonation. US Patent 6,712,342, March 20, 2004.

[18] Gabelman, A.; Hwang, S-T. Hollow Fiber Membrane Contactors. *J. Membr. Sci*. **1999**, *159*, 61.

APPENDIX A

Table A-1. Measured values of effluent seawater pH, cell current, voltage, and resistance as a function of time during two consecutive 59 minute polarity cycles at an applied cell current of 30 amps.

Sample	Time (minutes)	Current	Volts	Resistance	pH	Polarity
1	0	30	-	-		B
2	4	30	-	-		B
3	9	30	-	-		B
4	14	30	-	-		B
5	19	30	27.3	0.91	5.88	B
6	24	30	26.9	0.90	2.90	B
7	29	30	26.9	0.90	2.49	B
8	34	30	27.6	0.92	2.41	B
9	39	30	28.0	0.93	2.44	B
10	44	30	28.2	0.94	2.39	B
11	49	30	28.5	0.95	2.40	B
12	54	30	29.4	0.98	2.38	B
13	59	30	29.8	0.99	2.32	B
1	0	30	30.6	1.02	6.59	A
2	4	30	28.9	0.96	7.76	A
3	9	30	30.1	1.00	7.75	A
4	14	30	29.9	1.00	7.14	A
5	19	30	28.5	0.95	6.52	A
6	24	30	27.7	0.92	4.95	A
7	29	30	27.4	0.91	2.92	A
8	34	30	27.2	0.91	2.54	A
9	39	30	27.4	0.91	2.42	A
10	44	30	28.3	0.94	2.35	A
11	49	30	28.9	0.96	2.30	A
12	54	30	29.1	0.97	2.27	A
13	59	30	29.8	0.99	2.25	A

Table A-2. Measured values of effluent seawater pH, cell current, voltage, and resistance as a function of time during two consecutive 40 minute polarity cycles at an applied cell current of 30 amps.

Sample	Time (minutes)	Current	Volts	Resistance	pH	Polarity
1	0	30	31.5	1.09	7.09	B
2	5	30	29.4	0.98	7.92	B
3	10	30	30.0	1.00	7.82	B
4	15	30	29.7	0.99	7.07	B
5	20	30	27.9	0.93	6.23	B
6	25	30	26.6	0.89	3.27	B
7	30	30	26.7	0.89	2.63	B
8	35	30	27.0	0.90	2.46	B
9	40	30	27.2	0.91	2.38	B
1	0	30	28.9	1.00	7.33	A
2	5	30	28.9	0.96	7.84	A
3	10	30	29.6	0.99	7.60	A
4	15	30	28.1	0.99	6.47	A
5	20	30	27.4	0.91	3.90	A
6	25	30	26.8	0.89	2.68	A
7	30	30	26.6	0.89	2.46	A
8	35	30	27.3	0.91	2.35	A
9	40	30	27.5	0.92	2.30	A

Table A-3. Measured values of effluent seawater pH, cell current, voltage, and resistance as a function of time during two consecutive 40 minute polarity cycles at an applied cell current of 20 amps.

Sample	Time (minutes)	Current	Volts	Resistance	pH	Polarity
1	0	20	24.8	1.24	7.72	B
2	5	20	21.6	1.08	7.95	B
3	10	20	21.7	1.09	7.92	B
4	15	20	21.7	1.09	7.63	B
5	20	20	20.5	1.03	6.77	B
6	25	20	19.8	0.99	6.08	B
7	30	20	19.4	0.97	3.63	B
8	35	20	19.5	0.98	2.93	B
9	40	20	19.5	0.98	2.81	B
1	0	20	21.3	1.07	7.74	A
2	5	20	20.9	1.05	7.95	A
3	10	20	21.5	1.08	7.94	A
4	15	20	21.4	1.07	7.61	A
5	20	20	20.7	1.03	6.82	A
6	25	20	20.1	1.01	5.96	A
7	30	20	19.7	0.99	3.24	A
8	35	20	19.6	0.98	2.86	A
9	40	20	19.5	0.98	2.76	A

Table A-4. Measured values of effluent seawater pH, cell current, voltage, and resistance as a function of time during two consecutive polarity cycles at an applied cell current of 10 amps.

Sample	Time (minutes)	Current	Volts	Resistance	pH	Polarity
1	0	10	13.6	1.36	6.97	B
2	5	10	12.8	1.28	8.00	B
3	10	10	12.4	1.24	8.06	B
4	15	10	13.0	1.30	8.03	B
5	20	10	13.3	1.33	8.05	B
6	25	10	13.5	1.35	9.00	B
7	30	10	13.2	1.32	7.95	B
8	35	10	12.9	1.29	7.76	B
9	40	10	12.7	1.27	7.44	B
1	0	10	13.0	1.30	7.95	A
2	10	10	13.0	1.30	8.04	A
3	20	10	13.1	1.31	7.86	A
4	30	10	13.0	1.30	6.36	A
5	40	10	12.8	1.28	5.98	A
6	50	10	12.8	1.28	5.67	A
7	60	10	12.7	1.27	-	A

Table A-5. Measured values of effluent seawater pH, cell current, voltage, and resistance as a function of time during one 45 minute polarity cycles at an applied cell current of 20 amps.

Sample	Time (minutes)	Current	Volts	Resistance	pH	Polarity
1	0	20	25.6	1.28	7.90	B
2	5	20	22.7	1.14	8.01	B
3	10	20	23.5	1.18	7.97	B
4	15	20	23.5	1.18	7.80	B
5	20	20	22.5	1.13	6.77	B
6	25	20	21.5	1.75	6.22	B
7	30	20	20.9	1.05	5.18	B
8	35	20	20.8	1.04	3.11	B
9	40	20	20.8	1.04	2.72	B
10	45	20	20.7	1.04	2.69	B

Table A-6. Measured values of effluent seawater pH, cell current, voltage, and resistance as a function of time during two consecutive 45 minute polarity cycles at an applied cell current of 20 amps.

Sample	Time (minutes)	Current	Volts	Resistance	pH	Polarity
1	0	20	16.3	0.82	8.21	A
2	5	20	17.2	0.86	8.26	A
3	10	20	17.9	0.90	8.22	A
4	15	20	18.1	0.91	8.17	A
5	20	20	17.3	0.87	7.29	A
6	25	20	17.0	0.85	6.69	A
7	30	20	16.7	0.84	3.82	A
8	35	20	16.4	0.82	2.85	A
9	40	20	16.6	0.83	2.64	A
10	45	20	16.6	0.83	2.59	A
1	0	20	17.7	0.89	8.29	B
2	5	20	17.6	0.88	8.31	B
3	10	20	18.3	0.92	8.28	B
4	15	20	18.3	0.92	8.12	B
5	20	20	17.8	0.89	7.65	B
6	25	20	17.2	0.86	6.61	B
7	30	20	16.7	0.84	4.21	B
8	35	20	16.7	0.84	2.78	B
9	40	20	16.7	0.84	2.68	B
10	45	20	16.6	0.83	2.64	B

Table A-7. Measured values of effluent seawater pH, cell current, voltage, and resistance as a function of time during two consecutive 45 minute polarity cycles at an applied cell current of 20 amps.

Sample	Time (minutes)	Current	Volts	Resistance	pH	Polarity
1	0	20	17.0	0.85	7.72	A
2	5	20	17.2	0.86	7.62	A
3	10	20	18.1	0.91	7.58	A
4	15	20	18.0	0.90	7.52	A
5	20	20	17.5	0.88	6.99	A
6	25	20	16.9	0.85	6.66	A
7	30	20	16.5	0.83	6.03	A
8	35	20	16.4	0.82	3.01	A
9	40	20	16.3	0.82	2.77	A
10	45	20	16.2	0.81	2.70	A
1	0	20	17.5	0.88	7.56	B
2	5	20	17.8	0.89	7.72	B
3	10	20	18.6	0.93	7.73	B
4	15	20	18.1	0.91	7.59	B
5	20	20	17.6	0.88	6.99	B
6	25	20	16.8	0.84	6.58	B
7	30	20	16.5	0.83	4.79	B
8	35	20	16.1	0.81	2.92	B
9	40	20	15.9	0.80	2.71	B
10	45	20	16.1	0.81	2.62	B